

# UC San Diego

## UC San Diego Electronic Theses and Dissertations

### Title

Synthesis, Analysis, and Applications of Renewable Polyols

### Permalink

<https://escholarship.org/uc/item/83c2j946>

### Author

Tessman, Marissa Anne

### Publication Date

2016

Peer reviewed|Thesis/dissertation

UNIVERSITY OF CALIFORNIA, SAN DIEGO

Synthesis, Analysis, and Applications of Renewable Polyols

A Thesis submitted in partial satisfaction of the requirements  
for the degree Master of Science

in

Chemistry

by

Marissa Anne Tessman

Committee in charge:

Michael Burkart, Chair  
Stephen Mayfield  
Robert “Skip” Pomeroy

2016

Copyright

Marissa Anne Tessman, 2016

All rights reserved.

The Thesis of Marissa Anne Tessman is approved and it is acceptable in quality and form for publication on microfilm and electronically:

---

---

---

University of California, San Diego

2016

To my wonderful family who has given me nothing but support and love.

To AJ Pasaribu, who was always there for me, and who pushed me to achieve past what I thought I was capable of.

To my Grandma and Grandpa Whitten, who would be so proud to hear that his belief in the power of hard, smart work and investing in education has been passed to me.

## Table of Contents

Signature Page.....	iii
Dedication.....	iv
Table of Contents.....	v
List of Abbreviations.....	viii
List of Figures.....	x
List of Tables.....	xii
Acknowledgements.....	xiii
Abstract of the Thesis.....	xiv
Chapter 1: General Introduction.....	1
1.1 Introduction.....	1
1.2 Brief History and Background of Polyurethanes.....	2
1.3 Polyurethane Macrostructure.....	3
1.4 Polyols.....	4
1.5 Diisocyanates.....	7
1.6 Blowing Agents.....	9
1.7 Catalysts.....	10
1.8 Surfactants.....	12
1.9 References.....	12
Chapter 2: One-Pot Synthesis of Polyols from Algae Oil for Sustainable Polyurethanes.....	15
2.1 Abstract.....	15

2.2 Introduction.....	15
2.3 Experimental.....	17
2.3.1 Synthesis and Purification of Algae-Based Polyols.....	18
2.3.2 Characterization of Algae-Based Polyols.....	18
2.4 Results and Discussion.....	20
2.5 Conclusion.....	29
2.6 Acknowledgements.....	30
2.7 References.....	31
Chapter 3: Rigid Polyurethane Foam from Sustainable Polyols.....	32
3.1 Abstract.....	32
3.2 Introduction.....	33
3.3 Experimental.....	34
3.3.1 Pipe Mold Preparation.....	35
3.3.2 Prepolymer Preparation.....	36
3.3.3 Foam Pouring.....	37
3.3.4 Measuring Density and Hardness.....	37
3.4 Results and Discussion.....	37
3.5 Conclusion.....	44
3.6 Acknowledgements.....	44
3.7 References.....	45
Chapter 4: Eco Friendly Quality Analysis: A Greener Method for Measuring Polyol Hydroxyl Number Using FTIR-ATR Spectroscopy.....	47

4.1 Abstract.....	47
4.2 Introduction.....	47
4.3 Experimental.....	51
4.4 Results and Discussion.....	52
4.4.1 Characterization.....	52
4.4.2 Calibration.....	53
4.5 Conclusion.....	55
4.6 Acknowledgements.....	56
4.7 References.....	56

## List of Abbreviations

ASTM	American Society for Testing and Materials
ATR	attenuated total reflectance
CI	confidence interval
DA	Daltons
DG	diglycerides
DMAP	4- dimethylaminopyridine
FA	fatty acid
FAME	fatty acid methyl ester
FTIR	Fourier transform infrared
GCMS	gas chromatography mass spectrometer
GPC	gel permeation chromatography
HDI	1,6- hexamethylene diisocyanate
HRMS	high resolution mass spec
LCMS	liquid chromatography mass spectrometer
MDI	4,4'- methylene diphenyl diisocyanate
MG	monoglycerides
MSTFA	N-methyl-N-(trimethylsilyl)-trifluoroacetamide
MTBE	methyl tert-butyl ether
MW	molecular weight
NIR	Near infrared
NMP	N- methylpyrrolidone
NMR	nuclear magnetic resonance

PDI	pentamethylene diisocyanate
PDMS	polydimethylsiloxane
PU	polyurethane
QA	quality analysis
QC	quality control
TDI	2,4- toluene diisocyanate
T <sub>g</sub>	glass transition temperature
TG	triglycerides
TMP	trimethylolpropane

## List of Figures

Figure 1.1: Reaction between a polyol and an isocyanate to generate a urethane bond. The oxygen of the polyol's hydroxyl group is added to the carbonyl group within the isocyanate to produce an ester-amide.....	3
Figure 1.2: Example of foam cell structure.....	4
Figure 1.3: The polyurethane foam network between carbon chains, represented by the lines, and 2,4-toluene diisocyanate (TDI).....	6
Figure 1.4: 2,4- toluene diisocyanate (TDI, on top) and 4,4'-methylene diphenyl diisocyanate (MDI, on bottom).....	7
Figure 1.5: Catalytic nucleophilic addition elimination reaction mechanism between a polyol and an isocyanate to produce a urethane bond.....	10
Figure 1.6: The catalyzed reaction between water and an isocyanate is similar to that of a polyol, but the products are carbon dioxide, which causes the foam to expand, and an amine, which can react with another isocyanate.....	11
Figure 2.1: Prilezhaev epoxidation using per-acetic acid and ring opening using lactic acid.....	17
Figure 2.2: FTIR scans of one-pot polyol synthesis progressions over time using various acids. Clockwise from the top left: acetic acid epoxide, formic acid, acetic/propionic acid, acetic/lactic acid, lactic acid, and propionic acid.....	21
Figure 2.3: Algae oil FAME GC chromatogram and peak table.....	25
Figure 2.4: HRMS of propionic acid polyol and identification of a select group of peaks. P=oleic acid with a propionic substituent, D=oleic acid with dihydroxyl substituents. Approximate ranges of glycerides with decreasing chains have also been illustrated.....	27
Figure 2.5: HRMS of 1 pot acetic/propionic acid polyol and identification of a select group of peaks.....	28
Figure 3.1: Mold Setup.....	35

Figure 3.2: Core slice densities and hardness relative to position in the core.....	38
Figure 3.3: Average core density and hardness of four rigid foam samples...	39
Figure 3.4: Images of cells in representative core slices: surfboard (top left), control (top right), 28% algae (bottom left), and 36% soy surfboard (bottom right). The core slices were colored with blue ink before being photographed under a microscope at 10x scale.....	40
Figure 4.1: FTIR spectra of polyol standards from Agrol (left) and Honey Bee (right). Each spectrum has been normalized according to the baseline between 2200 and 1900 $\text{cm}^{-1}$ , and is labeled with its respective manufacturer-reported hydroxyl value.....	52
Figure 4.2: Calibration curves for Agrol (left) and Honey Bee (right) polyol standards.....	54

## List of Tables

Table 2.1: Carboxylic acids used to form polyols and their corresponding pKa.....	17
Table 2.2: Possible substituents attached during polyol synthesis.....	20
Table 2.3: Summary of FTIR peaks present in each polyol synthesis.....	22
Table 3.1: Materials and chemicals for rigid polyurethane. Polyols A, B, C, and J are the intellectual property of Arctic Foam.....	36

## Acknowledgements

I would like to acknowledge my TA Scott Wilson for his belief in my potential. It was this belief that first enabled me to work in a lab.

I would also like to acknowledge Dr. Robert “Skip” Pomeroy for his practical and unique approach to teaching, and for opening up his lab and allowing me to work independently. This has shaped my entire approach to chemistry, education, and life.

Lastly, I would like to acknowledge everyone in Skip’s lab who has supported me in my projects. You have made the last two years so enjoyable!

Chapter 2, in full, is a reprint of material being prepared for publication. Tessman, Marissa; Lee, Yi-Che; Hartel, Nicolas; Talan, Griffin; Bonilla, Brandon; Ramos, Joshua; Burkart, Michael D.; Pomeroy, Robert. 2016. The thesis author was the primary investigator and author of this paper.

Chapter 4, in full, is a reprint of material currently submitted for publication. Tessman, Marissa; Burkart, Michael; Pomeroy, Robert. “Eco Friendly Quality Analysis: A Greener Method for Measuring Polyol Hydroxyl Number Using FTIR-ATR Spectroscopy”, 2016. The thesis author was the primary investigator and author of this paper.

ABSTRACT OF THE THESIS

Synthesis, Analysis, and Applications of Renewable Polyols

by

Marissa Anne Tessman

Master of Science in Chemistry

University of California, San Diego, 2016

Professor Michael Burkart, Chair

Renewable polymers have been of increasing interest as replacements for petroleum based products. Here, an efficient, one-pot method of synthesizing renewable, sustainable, and biodegradable polyols from algae oil was developed, demonstrating that Prilezhaev epoxidation with acetic acid and ring-opening with short-chain carboxylic acids can be performed in a single step. Renewable polyols from MCPU Engineering were utilized to create a rigid polyurethane foam surfboard with a weight-by-weight percent renewability of 11%. Though this foam did not have the same density or hardness of a benchmark board, the cause of this was determined to be due to additive and processing differences rather than inferior polyols. Tests manipulating the additives and foam pouring process are currently underway. A method of measuring polyol hydroxyl number to within 5% using Fourier Transform infrared spectroscopy was also developed, which presented a faster, less expensive, and more environmentally-conscious alternative to current methods.

## Chapter 1: General Introduction

### 1.1 Introduction

As of 2013, the global polyurethane (PU) industry produced over 11 million tons annually.<sup>1</sup> PU spans a broad range of applications, appearing in rigid and soft foams, elastomers, coatings, thermoplastics, thermosets, and fibers, to name a few categories.<sup>2</sup> Practical examples include seat cushioning, home insulation, rubber, protective coatings for floors and cars, footwear, and fabric such as Spandex or faux leather. Although one of the most prevalent and frequently-used materials, PUs are almost entirely non-renewable, non-sustainable, non-biodegradable, and have limited recyclability, meaning that among the 11 million tons generated per year, a large majority is disposed of as waste after being used. Typically, almost every part of the polyurethane process contains some toxic and/or petroleum-based chemical, contributing to rising global fossil fuel consumption. The introduction of a more environmentally friendly process or chemical to any part of polyurethane production will have a dramatic effect on the entire industry.

This thesis presents three research projects designed as green alternatives to the current industry. The first chapter outlines a brief history of polyurethanes and details its synthesis and macrostructure. The second chapter describes a novel, one-pot synthesis and characterization of algae-based polyol, one of two major components in PU. The third chapter details the creation of rigid PU foam from algae and soy-based polyols rather than petroleum. The fourth and final chapter provides an alternative to the current method for measuring polyol hydroxyl number, a quantity describing the

amount of hydroxy groups present per gram of polyol currently measured using a slow, expensive, and toxic technique.

## 1.2 Brief History and Background of Polyurethanes

Polyurethanes and the petroleum industry have grown hand in hand. PU development first occurred in Germany in the early 1900's, where the isocyanate molecule known as 1,6-hexamethylene diisocyanate (HDI) was first synthesized by Heinrich Rinke of the Bayer Corporation in 1937. Otto Bayer himself developed the polyurethane reaction process in that same year. Beginning in 1940, these new polymers were initially conscripted to replace expensive and less durable natural rubbers used by the Germans at alarming rates during World War II. Post war, companies such as Goodrich and DuPont expanded on the initial research, but it wasn't until the 1970's that the polyurethane market gained momentum, dominated by Bayer, BASF, and Dow, among others.<sup>3</sup> PU is just one early example of a polymer developed from these petroleum-based companies. Other plastics such as polyethylene developed alongside PU as processing methods and structural understanding improved.<sup>4</sup> After early breakthroughs in petro-polymers, natural polymer synthesis stagnated, leading to a major knowledge gap that continued to grow for the remainder of the century.<sup>5</sup> Only recently has uncertainty in the oil market and climate change findings renewed interest in renewable, sustainable, and biodegradable polymers.

Polyurethanes are created from two major components: a polyol, and an isocyanate, as seen in Figure 1.1. During polymerization, the hydroxyl groups (OH) react with the isocyanate groups ( $\text{N}=\text{C}=\text{O}$ ) to produce urethane bonds. Note how there

can be  $n$  functional groups on each molecule. This allows them to react with more than one molecule to produce a network in a reaction known as crosslinking. The resulting polyurethane can be thought of as a single, high molecular weight (MW) molecule comprised of rigid urethane bonds between long, flexible carbon chains, known as hard and soft segments, respectively.<sup>6</sup>

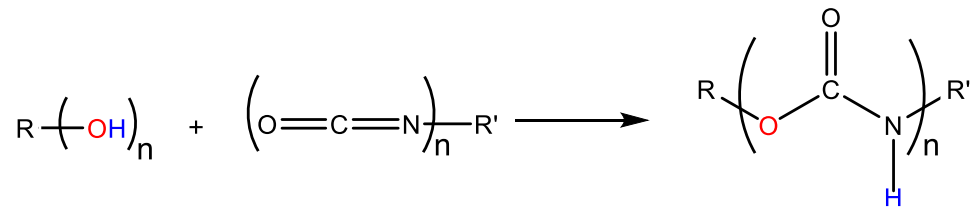


Figure 1.1: Reaction between a polyol and an isocyanate to generate a urethane bond. The oxygen of the polyol's hydroxyl group is added to the carbonyl group within the isocyanate to produce an ester-amide.

### 1.3 Polyurethane Macrostructure

Polyurethane foam formation consists of four major steps: bubble generation, bubble packing and stabilization, polyurethane stiffening and cell opening, and curing. Bubbles are formed through a combination of mechanical mixing, when the polyol components are added to the isocyanate, and the introduction of a blowing agent that produces gas within the foam (see Section 1.6 Blowing Agents). As the foam reaction progresses, the heat released causes the bubbles to expand and pack against each other into polyhedral forms (Figure 1.2). During this step, fluid drains from the cell walls into the interfaces (or struts) joining multiple bubbles together, in a mechanism known as the Marangoni Effect. The struts begin to stiffen and support the weight of the foam. Thin walls exist between the bubbles, resulting in a closed cell foam, unless the

cell walls reach a critical pressure and burst. During the curing stage, the PU reaction slowly completes. This can be aided by placing the foam in an oven. Curing produces a significant change in mechanical properties including Shore Hardness, flexibility, and compressive strength.<sup>18</sup>

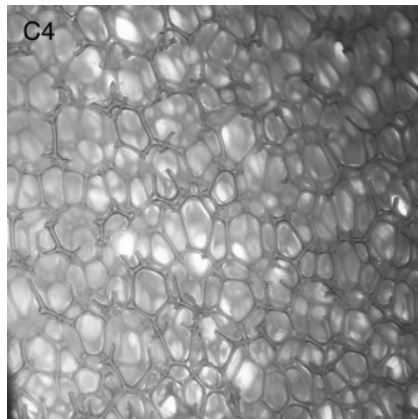


Figure 1.2: Example of foam cell structure

#### 1.4 Polyols

Polyols are classified as any molecule with two or more hydroxyl groups. These functional groups react with isocyanate groups to form urethane bonds in polyurethane foams. Consequently, the hydroxyl number, carbon chain length, functionality, and substitution dramatically influence the rate and degree of reactivity, and the microstructure, which, in turn, affects macroscopic structure and performance.

Hydroxyl number refers to the weight equivalence of OH groups, calculated via the following equation:

$$\text{Hydroxyl Number} = \text{mg KOH/g polyol}$$

Hydroxyl number is measured via acetylation of the OH groups with acetic anhydride, and titration of the side product, acetic acid, with potassium hydroxide (ASTM D4274).<sup>7</sup> Hydroxyl number is extremely important in the selection of polyols for specific applications. In a series of similar polyols with increasing hydroxyl numbers, larger hydroxyl numbers will produce more urethane bonds, and will therefore exhibit more hardness. There are two methods of affecting the hydroxyl number of a polyol: changing its molecular weight, or manipulating its functionality. The former involves selecting or synthesizing reactants of different sizes, and the latter involves adjusting the number of OH groups per molecule. A molecule such as 1,4-butanediol, for example, has a low molecular weight of 90 g/mol, but because it is di-functional it has a high hydroxyl number of 1245 mg KOH/g polyol.

The number of carbons between hydroxyl groups also affects flexibility. Longer chain polyols ranging in molecular weight from 100 to 2000 g/mol contribute more flexibility, and generally serve as the primary polyol component in a foam. Short-chain polyols such as 1,4-butanediol, trimethylolpropane (TMP), and glycerol are referred to as crosslinkers, because they connect two isocyanate molecules in close proximity, creating larger hard segments. They are also referred to as chain-extenders, a name derived from the PU foam manufacturing process. Generally, long-chain polyols are pre-mixed with an excess of diisocyanate, producing lengthy polymers capped by unreacted isocyanate groups. The short-chain polyols are then added, which react with the terminal isocyanates and connect the pre-mixed polymers together, as demonstrated in Figure 1.3.<sup>8</sup> Branched polyols also affect the foam's physical properties, reducing the flexibility of the soft polyol segments.

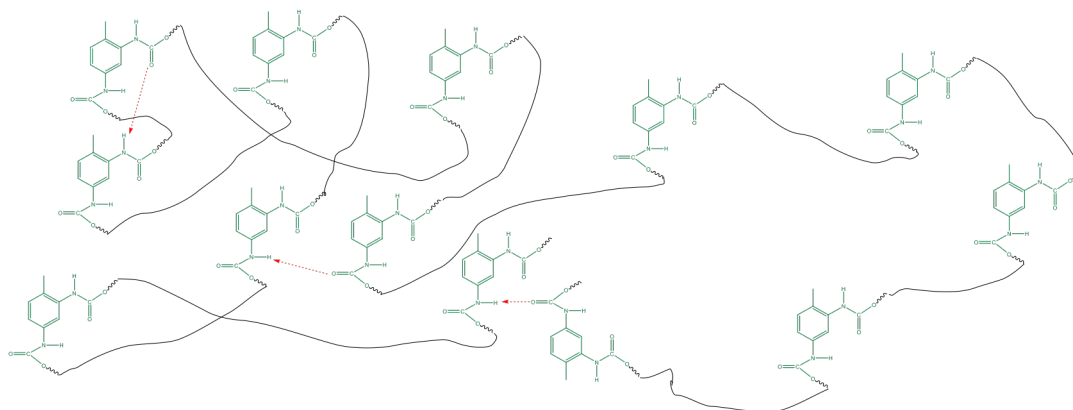


Figure 1.3: The polyurethane foam network between carbon chains, represented by the lines, and 2,4-toluene diisocyanate (TDI). Longer chains create distance between TDI molecules, leading to low cross-linking density and softer, more flexible foams. Short chains, as seen in the upper left, increase cross-linking density, leading to larger hard segments and stiffer foams. The arrows depict hydrogen bonds between different urethane bonds.

The final major factor affecting polyol reactivity is the substitution of the hydroxyl groups along the carbon chains. Primary hydroxyl groups react more rapidly than their secondary counterparts. Reaction speed has implications for both the resulting product and the type of production process used. Polyurethanes exhibit varying stages of hardening throughout the course of the reaction, the first of which is the “cream time”, where the mixture’s viscosity increases dramatically. An overly rapid cream time can result in layering patterns and air pockets as the mixture is poured into a mold. On the other hand, too slow of a cream time can result in an incomplete reaction, or macrophase separation between the hard and soft segments, both of which can decrease the foam’s mechanical properties and robustness.<sup>9</sup>

Among oil-based polyols, polydispersity plays a role in determining PU physical characteristics. Most petroleum-based polyol structures are highly regular with small differences in MW. Polyols with greater structural irregularity and a higher MW distribution tend to also produce greater PU hard and soft segment size distribution and irregular segment incompatibility, which leads to inferior mechanical properties.<sup>9,14,15</sup>

### 1.5 Diisocyanates

Diisocyanates contain two isocyanate groups. The two most commonly used diisocyanates are 2,4- toluene diisocyanate (TDI) and 4,4'-methylene diphenyl diisocyanate (MDI), shown in Figure 1.4, which are synthesized through the phosgenation of their respective diamine precursors.<sup>10</sup>

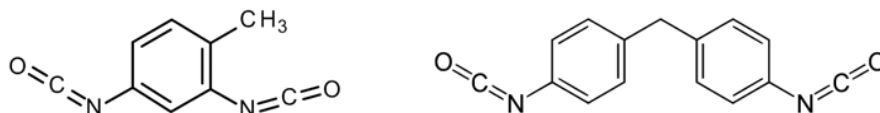


Figure 1.4: 2,4- toluene diisocyanate (TDI, left) and 4,4'-methylene diphenyl diisocyanate (MDI, right).

PU generally contains between 50 and 70% diisocyanate by weight, making the petroleum-based chemical a large fraction of the foam industry's petrochemical consumption. Researchers have toyed with the idea of creating renewable, linear diisocyanates since 2010, using lipids as natural precursors.<sup>11</sup> As recently as 2015, Bayer MaterialScience developed pentamethylene diisocyanate (PDI), a 70%

renewable diisocyanate.<sup>12</sup> Little headway has been made in the production of renewable, aromatic diisocyanates. Although naturally-based diisocyanates would substantially increase PU renewability, the molecules themselves exhibit health concerns. Long-term exposure causes sensitivity and irritation to the lungs and eyes, and eventual respiratory failure. Respirators, goggles, and gloves must be worn at all times when handling these reactants, and they must be disposed of as toxic waste. MDI is the least toxic of the diisocyanates as it has a low vapor pressure and exists at room temperature as a solid. TDI, on the other hand, has a higher vapor pressure, and has been the topic of a number of workplace injuries and illnesses. When reacted with polyols, however, the conversion of isocyanate groups to urethane bonds renders the molecule stable and non-toxic. Toxicity concerns have prompted some researchers to find alternative PU reactants.

Because of their polarity, urethane bonds, or hard segments, tend to be physically incompatible with the non-polar, long-chain polyols, or soft segments. Thus, in a PU mixture, N-H  $\cdots$  O=C intermolecular hydrogen bonds facilitate the grouping of hard segments into larger hard domains suspended within an amorphous soft segment matrix, known as the soft domain (Figure 1.3).<sup>13</sup> The hard domains exhibit a higher glass transition temperature ( $T_g$ ) than the soft domains, giving them a crystalline structure and allowing them to act as reinforcement. Any feature that disrupts the ability of the hard segments to act as reinforcement decreases the rigidity and durability of the foam. Foam quality depends on hard segment concentration, size distribution, and segregation from the soft domains. Higher concentration leads to greater crystalline density within the soft domain, which exhibits more thermal

stability and rigidity, but less flexible foam. A large size distribution between hard domains also contributes to less durable foam. Physical segregation between the hard and soft domains also plays a role, as hard domains that are semi-amorphous due to partial mixing with the soft domains lose their reinforcing properties.<sup>9,14,15</sup>

## **1.6 Blowing Agents**

Blowing agents added to a PU reaction mixture form bubbles and facilitate foam rising. They are classified as either non-reactive or reactive. The non-reactive blowing agents evaporate throughout the course of the reaction due to either the exothermicity of the PU reaction, or to the physical heating of the foam during the production process. Pentane is a common non-reactive blowing agent. A reactive blowing agent undergoes a chemical reaction within the mixture to produce a gas. Water is the most common reactive blowing agent, as it reacts with isocyanate groups to produce carbon dioxide and an amine. Uncatalyzed, the reaction proceeds fairly slowly at room temperature, forming amines that crosslink with excess isocyanates to form a network of solid urea bonds, further slowing the rate by forming a physical barrier between reactants. The catalyzed reaction, on the other hand, proceeds on the order of minutes, and is highly exothermic. While speed is desired when forming a mechanically-superior foam, the temperature gradient between the center and surface of the foam due to the reaction's exothermicity can lead to structural incompatibilities, shrinking, and thermal discoloration.<sup>16</sup> Thus is it necessary to control both the urethane and carbon dioxide reactions through the use of catalysts.

## 1.7 Catalysts

The uncatalyzed reaction between polyols and diisocyanates is extremely slow, taking hours to complete, so to produce any kind of timely rise and gel, catalyst addition is essential.<sup>6</sup> There are two major types of catalysts, referred to here as the gel and water catalysts. Most of these catalysts are tertiary amines, although some metal catalysts have been used as well.<sup>6,17</sup>

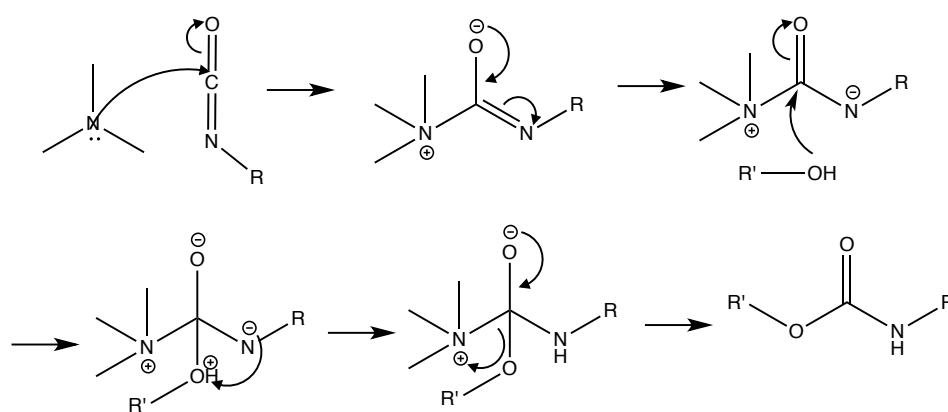


Figure 1.5: Catalytic nucleophilic addition-elimination reaction mechanism between a polyol and an isocyanate to produce a urethane bond. The addition of the catalyst to the carbonyl carbon of the isocyanate lowers the activation energy of the reaction by serving as a good leaving group.

The gel catalyst facilitates the reaction between the polyol and diisocyanate. The exact mechanism for this catalyst-assisted reaction is still unknown, though the most widely accepted one is depicted in Figure 1.5. In this mechanism, the nucleophilic tertiary amine attacks the electrophilic carbonyl carbon in the isocyanate to produce a urea intermediate. The electrophilic hydroxyl group can then attack the carbonyl carbon and remove the catalyst in a nucleophilic addition/elimination

reaction, as  $\text{NR}_3^+$  is an excellent leaving group. The catalyst is restored, and the urethane bond is formed.

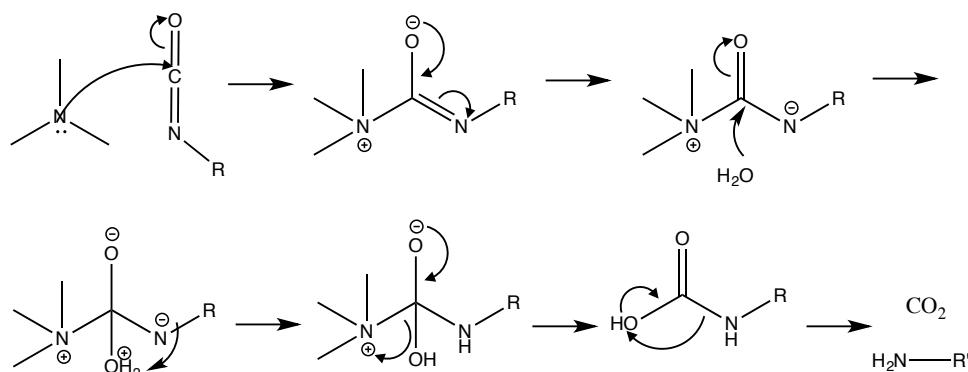


Figure 1.6: The catalyzed reaction between water and an isocyanate is similar to that of a polyol, but the products are carbon dioxide, which causes the foam to expand, and an amine, which can react with another isocyanate.

The water catalyst facilitates the reaction between water and diisocyanate. The mechanism is thought to be similar to that of the gel reaction, with water acting in place of the polyol. The difference occurs after water is added to the carbonyl carbon of the isocyanate, and the amine catalyst is displaced. The product of this step is a carbamic acid, which undergoes decarboxylation to produce carbon dioxide gas and a primary amine (Figure 1.6). The amine functions similarly to a primary polyol, and can undergo further reactions, although these reactions have been shown to have little effect on the foam.<sup>16</sup> The carbon dioxide escapes as a gas, causing the foam to expand as it does so- analogous to the reaction in which bread rises.

Although most catalysts are not exclusive to either reaction, catalysts classified as water catalysts contain a similar feature: an ether located gamma to the tertiary

amine. The mechanism behind why this structure favors the water-isocyanate reaction is currently unknown.<sup>6</sup>

## 1.8 Surfactants

Surfactants control two aspects of polyurethane process, formula immiscibility and cell expansion. Due to the physical incompatibility of the isocyanates and polyols, surfactants emulsify the mixture to encourage miscibility. The most generic surfactants consist of a polydimethylsiloxane (PDMS) backbone attaching polyether side chains.<sup>18</sup> The PDMS is relatively polar, while the polyether side chains are relatively nonpolar, functioning as an interface for both the isocyanates and polyols. Along the cell walls, silicone surfactants also reduce surface tension, slowing fluid drainage, and preventing the cells from bursting prematurely.<sup>18</sup>

## 1.9 References

1. (2013). Polyurethanes. *The Essential Chemical Industry*. York, United Kingdom: University of York. Retrieved from <http://www.essentialchemicalindustry.org/polymers/polyurethane.html>
2. Ionescu, M. (2005). *Chemistry and Technology of Polyols for Polyurethanes*. Shawbury, Shrewbury, Shropshire, United Kingdom: Rapra Technology.
3. Prisacariu, C. (2011). *Polyurethane Elastomers: From Morphology to Mechanical Aspects*. Wien New York: Springer.
4. Reiche, B. (1949). Poly-The All-Star Plastic. *Popular Mechanics* 91 (1), 125-129. Retrieved 18 November 2016.
5. Travis, A. S., Schroter, H. G., Homburg, E., & Morris, P. J. T. (Eds.). (1998). *Determinants in the Evolution of the European Chemical Industry, 1900-1939: New Technologies, Political Frameworks, Markets and Companies*. Springer-Science & Business Media.

6. Sonnenschein, M. (2015) Theoretical Concepts and Techniques in Polyurethane Science. *Polyurethanes: Science, Technology, Markets, and Trends* (127-159). Hoboken, New Jersey: Wiley.
7. ASTM D4274-11, 2011, "Standard Test Methods for Testing Polyurethane Raw Materials: Determination of Hydroxyl Numbers of Polyols," ASTM International, West Conshohocken, PA, 2011, DOI: 10.1520/D4274-11, [www.astm.org](http://www.astm.org).
8. Kapps, M., & Buschkamp, S. (2004). The production of rigid polyurethane foam. *Insulation Technology Information*, Bayer MaterialScience, File no: PU21012-0406 en, 1-46.
9. He, Y., Xie, D., & Zhang, X. J. (2014). The structure, microphase-separated morphology, and property of polyurethanes and polyureas. *J Mater Sci*, 49 (21), 7339-7352.
10. Six, C., & Richter, F. (2005). "Isocyanates, Organic", *Ullmann's Encyclopedia of Industrial Chemistry*, Weinheim: Wiley-VCH, doi:[10.1002/14356007.a14\\_611](https://doi.org/10.1002/14356007.a14_611)
11. Hojabri, L., Kong, X., & Narine, S.S. (2010). Functional thermoplastics from linear diols and diisocyanates produced entirely from renewable lipid sources. *Biomacromolecules*, 11(4), 911-918.
12. Rothbarth, F. (2015, January 15). New milestones in polyurethanes. *Bayer MaterialScience at the European Coatings Show 2015 in Nuremberg*. Retrieved from: <http://www.press.bayer.com/baynews/baynews.nsf/id/9SSDPM-New-milestones-in-polyurethanes>
13. Blackwell J., Nagarajan M. R., & Hoitink T. B. (1981). The Structure of the Hard Segments in MDI/diol/PTMA Polyurethane Elastomers. *Urethane Chemistry and Applications*, 179-196. DOI:10.1021/bk-1981-0172.ch014
14. Klinedinst, D.B., Yilgör, I., Yilgör E., Zhang, M., & Wilkes G.L. (2012). The effect of varying soft and hard segment length on the structure-property relationships of segmented polyurethanes based on a linear symmetric diisocyanate, 1,4-butanediol and PTMO soft segments. *Polymer* 53, 5358-5366.
15. Chen, K.S., Yu, T.L., Chen, Y.S., Lin, T.L., & Liu, W.J. (2001). Soft- and Hard-Segment Phase Segregation of Polyester-Based Polyurethane. *J. Polym. Res.*, 8(2), 99-109.
16. Eaves, D. (2004). *Handbook of Polymer Foams*. Shawbury, Shrewbury, Shropshire, United Kingdom: Rapra Technology.

17. Forrest, M. J. (1999). *Chemical Characterisation of Polyurethanes*. Shawbury, Shrewbury, Shropshire, United Kingdom: Rapra Technology.
18. Zhang, X. D., Macosko, C. W., Davis, H. T., Nikolov, A. D., & Wasan, D. T. (1999). Role of Silicone Surfactant in Flexible Polyurethane Foams. *Journal of Colloid and Interface Science*, 215, 270-279.

## **Chapter 2: One-Pot Synthesis of Polyol from Algae Oil for Sustainable**

### **Polyurethanes**

#### **2.1 Abstract**

Renewable polymers have been of increasing interest as replacements for petroleum based products, and algae biomass offers distinct benefits as renewable resources that do not compete with food production. We have developed new one-pot methods for the conversion of algae oils into polyols for application to the production of rigid polyurethanes. Here we outline the initial research into the optimization of this procedure that employs small organic acids with hydrogen peroxide for a tandem epoxidation – ring opening that occurs in a single reaction sequence. We apply oils sourced from microalgae to provide a sustainable application of green chemistry for commercially relevant products. The methodology developed here provides a renewable source of urethane components that is more rapid, less expensive, and use less toxic precursors than previously published methods for the conversion of triglycerides to polyol.

#### **2.2 Introduction**

Current global trends of climate change caused by carbon emissions from fossil fuels are encouraging many chemical industries, especially those that rely heavily on petroleum products, to investigate more sustainable manufacturing processes.<sup>1</sup> A large sector with potential for improvement is the polyurethane (PU) industry, which produces versatile polymers and foams for use in many commercial products, from foams to thermoplastics. PU foams are employed in a wide variety of

industrial applications, including, but not limited to their use in flexible cushions, elastomers, coatings, and insulation.<sup>2</sup> Production of these polymers is dependent on precursor “polyols”, or long-chain hydrocarbons with hydroxyl groups along the carbon backbone. These polyols are condensed with di- or poly-isocyanates to produce PU foam, and varying the identity of these basic monomers provides the broad variety of PU products. Current production of industrial polyols is dominated by petroleum-derived polyethers, which are unsustainable and present environmental hazards due to their poor degradation in the environment.<sup>3</sup> The fact that the global PU market depends on a continuously dwindling petroleum supply also begets the impetus to search for renewable PU sources.

Recent work by Monteavaro *et al.* has shown that polyols can be produced from plant based oils, or triglycerides (TG), via the epoxidation of unsaturated hydrocarbon bonds.<sup>4</sup> TG that consists of unsaturated fatty acids such as oleic, linoleic and linolenic acids, often found in many plant and algae oils, contain at least one unsaturation available for epoxidation using the Prilezhaev reaction. In these reactions, TG is commonly epoxidized with a peroxy acid, followed by ring opening with an appropriate nucleophile (Figure 2.1).<sup>5</sup> While organic acids have been used to prepare peroxyacids with hydrogen peroxide for this epoxidation,<sup>6</sup> and organic alcohols have been demonstrated in epoxide ring opening,<sup>7,8</sup> these two concepts have not been combined into a simplified, one-step method.

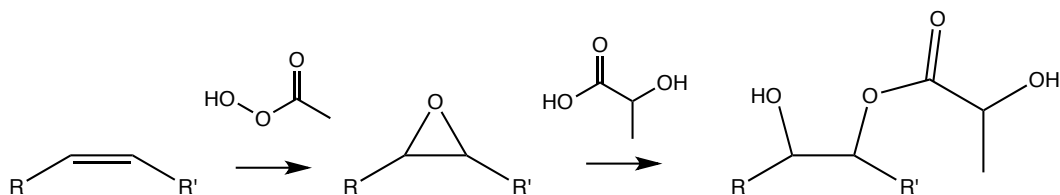


Figure 2.1: Prilezhaev epoxidation using per-acetic acid and ring opening using lactic acid

In an effort to develop methods for algae sourced TG, we desired a rapid process that could be performed on a variety of scales with a minimum number of steps. We show how small hydroxy acids and hydrogen peroxide can be used for a tandem epoxidation—ring opening in a one pot protocol that provides polyols appropriate for the preparation of rigid polyurethanes. Using algae TG, we evaluate a panel of organic acids for suitability in this procedure and subsequently prepare polyurethanes from the polyol products.

### 2.3 Experimental

One-pot methods using four different carboxylic acids in algal oil (Table 2.1) were compared to one-pot syntheses in which acetic acid was added to supplement the carboxylic acid reaction by forming epoxides in-situ.

Table 2.1: Carboxylic acids used to form polyols and their corresponding pKa.

Acid Name	Formic	Lactic	Acetic	Propionic
Chemical Structure				
pKa	3.75	3.86	4.75	4.87

### 2.3.1 Synthesis and Purification of Algae-Based Polyols

Stoichiometric equivalents of Soleum™ VHO algae oil, glacial acetic acid, and the acids featured in Table 2.1 were vigorously stirred and preheated to 75 °C in a reflux apparatus. Upon reaching thermal equilibrium, hydrogen peroxide was added dropwise for 30 minutes. Once the peroxide had been added, the reaction was left to stir and heat for 6+ hours. Reaction progression was accompanied by a whitening of the solution and an increase in viscosity. The top polyol layer was transferred into a separatory funnel. MTBE was added to decrease the viscosity enough to promote clean separation of the aqueous and organic layers, and the mixture was neutralized with a warm, saturated sodium bicarbonate solution until the top layer tested neutral to slightly basic with pH paper. After removing as much of the bottom layer as possible, neutralized polyol was heated at 55 °C to remove the MTBE, and then at 110 °C until the sample stopped bubbling to remove trace water.

### 2.3.2 Characterization of Algae-Based Polyols

#### *FTIR Spectroscopy*

At regular intervals during the synthesis, a small sample was extracted, neutralized, and dried according to the previous step. The pure polyol was scanned 10 times at a 1 cm<sup>-1</sup> resolution on a Perkin Elmer Spectrum X FTIR spectrometer to test for reaction completion.

#### *GCMS*

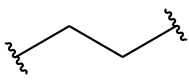
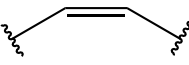
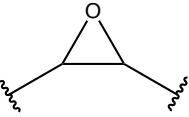
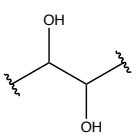
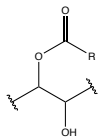
A sample of algae oil and was broken into fatty acid methyl esters through an acid-catalyzed transesterification reaction. 10 g of oil, 6 g of methanol, and 6.6 g of

0.77 mol/kg sulfuric acid in methanol were refluxed at variable temperatures between 25 °C and 115 °C over 48 hours. The product was neutralized with sodium bicarbonate dissolved in methanol. A 0.1 g sample was then transferred to a GCMS vial, combined with 0.05 g of a 1 g/L solution of 1,2,4 butanetriol in pyridine as an internal standard, and derivatized with 0.1 g of N-methyl-N-(trimethylsilyl)-trifluoroacetamide (MSTFA). After waiting 20 minutes for derivatization completion, the sample was diluted to 1.5 mL with pentane and analyzed on an Agilent 7820A/5975 GC/MS using a 25 m x 320  $\mu$ m x 1  $\mu$ m BP5 5%phenyl dimethyl polysiloxane column with a split ratio of 25:1 and the inlet temperature at 250 °C. The oven temperature was held at 100 °C for 4 minutes, then increased to 200 °C at 10 °C/min and held for 5 minutes, followed by an increase to 200 °C at 5 °C/min and a hold for 15 minutes.

#### *Ultra-High-Resolution MS*

The propionic and acetic/propionic polyols were saturated in acetonitrile and injected into an Electrospray/Orbitrap MS using FIA. The solvent system was 5 mM ammonium acetate in acetonitrile, and had a flow rate of 0.1 mL/min. The samples were detected using a +eV full scan between 150 and 2000 m/z. The sample peak appeared between 0.29 and 2.78 minutes, and the m/z abundances within that range were averaged and displayed on a single mass spectrum. The high resolution enabled identification of substituents added to the oleic double bond during polyol synthesis with a 0.005 Da accuracy. Table 2.2 shows the structures of the oleic acid 9-10 carbons most likely to be identified. The mass spectrum also identified the extent to which the triglycerides were broken during synthesis.

Table 2.2: Possible substituents attached during polyol synthesis

Substituent	Oleic Structure (9-10 carbons)	Reaction
Saturated		N/A
Unreacted double bond		No reaction
Epoxide		Prilezhaev epoxidation
dihydroxyl		Nucleophilic addition of water
Carboxylic acid		Nucleophilic addition of carboxylic acid

## 2.4 Results and Discussion

Each organic acid was subjected to two different reactions: a one-pot synthesis and a one-pot synthesis accompanied by acetic acid, which has been shown to promote epoxide formation.<sup>6</sup> The purpose of testing these two reactions was to determine the role of pKa/acid chain length, acid substituents in polyol and epoxide formation, and the degree to which acetic acid also functioned as a ring-opener. The algae oil was derivatized and tested using GCMS to analyze fatty acid content and to assist in the identification of specific polyol compounds using HRMS. Each reaction product was also analyzed by FTIR spectroscopy.

### FTIR Spectroscopy

Each polyol was analyzed by FTIR for either the formation of a polyol, as indicated by the appearance of an OH peak at  $3400\text{ cm}^{-1}$ , or the appearance of an epoxide, as indicated by the peak at  $830\text{ cm}^{-1}$ . The disappearance of the C=C peak at  $3000\text{ cm}^{-1}$  implied either reaction.

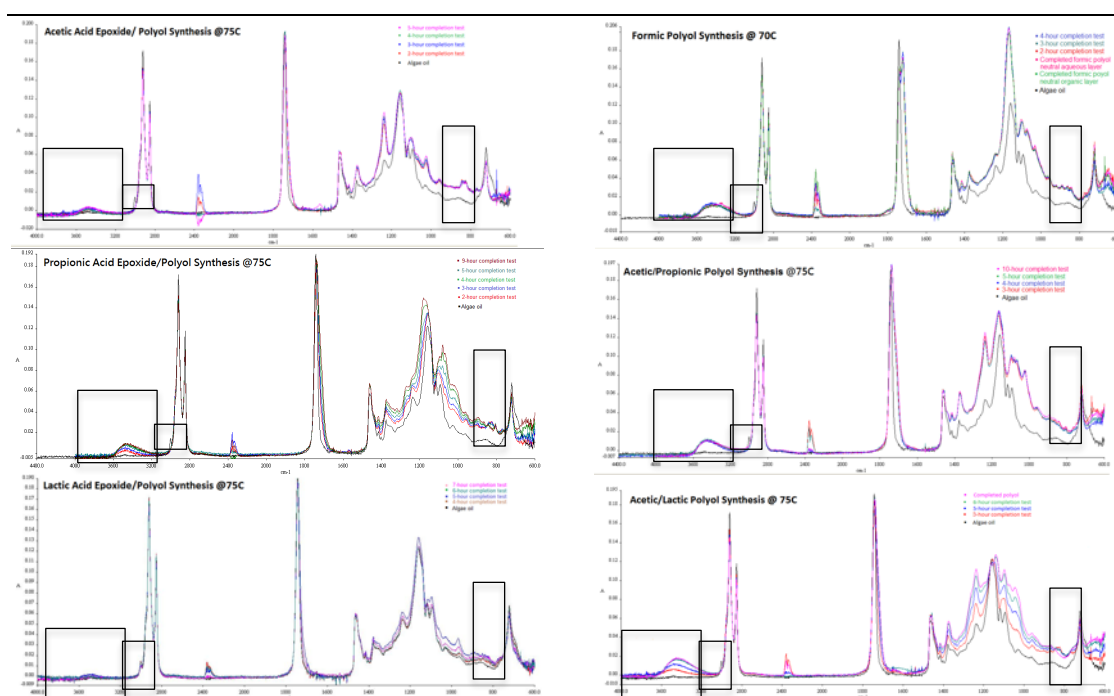


Figure 2.2: FTIR scans of one-pot polyol synthesis progressions over time using various acids. Clockwise from the top left: acetic acid epoxide, formic acid, acetic/propionic acid, acetic/lactic acid, lactic acid, and propionic acid. Scans were compared to unreacted algae oil. Peaks indicating reaction progression are boxed (OH:  $3400\text{ cm}^{-1}$ , C=C-H:  $3000\text{ cm}^{-1}$ , epoxide:  $830\text{ cm}^{-1}$ ).

Based on observation of the above peaks in each reaction's FTIR spectrum, the acetic acid formed both epoxides and polyol (Figure 2.2, top left), while the formic acid formed a polyol with no observable residual epoxides (Figure 2.2, top right). The propionic acid (Figure 2.2, middle left) and propionic/acetic acid (Figure 2.2, middle

right) reactions both formed polyols as seen by the OH peaks in both spectra, although the propionic acid polyol spectrum also contained an epoxide peak, implying incomplete conversion from epoxide to polyol. A comparison of the lactic acid (Figure 2.2, bottom left) and the lactic/acetic acid spectra (Figure 2.2, bottom right) demonstrated that little epoxidation occurred without the presence of acetic acid. In the lactic acid epoxide spectrum, the C=C peak was present and the epoxide peak was absent, whereas in the lactic/acetic spectrum, both the C=C and epoxide peaks were absent and a strong OH peak had appeared (Figure 2.2, bottom). The fingerprint regions were also noticeably different. The results are summarized in Table 2.2.

Table 2.3. Summary of FTIR peaks present in each polyol synthesis.

Acid Type	C=C	OH	Epoxide	Summary
Formic	X	✓	X	Complete polyol formation
Lactic	✓	X	X	No epoxidation or polyol formation
Acetic	X	✓	✓	Epoxidation, little to no polyol formation
Propionic	X	✓	✓	Epoxidation, incomplete polyol formation
Acetic/Lactic	X	✓	X	Complete polyol formation
Acetic/Propionic	X	✓	X	Complete polyol formation

FTIR analysis negates the hypothesis that only carboxylic acid pKa governs epoxidation and polyol synthesis. Under identical thermal conditions, formic acid, propionic acid, and to a lesser extent, acetic acid, formed at least some polyol after 3 hours, while lactic acid, with a pKa between that of formic and acetic acid, did not form an epoxide at all. Among the carboxylic acids with only single carbon differences, formic acid reacted significantly faster than both acetic and propionic acid, leading to the conclusion that pKa increases due to the addition of carbon

influences reaction rate. However, the addition of a substituent to the chain seemed to halt epoxide formation despite a lower pKa, as demonstrated in the comparison between propionic and lactic acid, which differ only by the presence of a hydroxyl group alpha to the carbonyl. Lactic acid has a lower pKa than propionic acid, but no reaction was apparent on its FTIR spectrum. The hydroxyl group may prevent the formation of a peroxyacids or undergo intramolecular hydrogen bonding with the peroxy-hydrogen, stabilizing the unreactive conformer and preventing Prilezhaev epoxidation. However, further research must be performed to test these hypotheses.

The presence of acetic acid in the one pot procedure increased reaction rate in the propionic acid reaction and promoted epoxidation in the lactic acid reaction, allowing polyol synthesis to occur as well. In the middle spectra in Figure 2.2, the propionic/acetic reaction completed polyol formation in just 3 hours, compared to 4 to 5 hours when the acetic acid was not present. The increase in reaction rate was most likely due to the addition of an acid with a lower pKa, a trend noted in the single-acid reactions (see previous paragraph). In the case of the lactic/acetic acid reaction, acetic acid promoted epoxidation when the lactic acid could not, a trend clearly seen in the contrast between the OH peaks in both bottom spectra in Figure 2.2. Once the oil was epoxidized, lactic acid was able to open the ring at a faster rate than acetic acid, resulting in completed polyol after 6 hours.

### *GCMS*

GCMS was performed to analyze the fatty acid content of the oil used in all polyol syntheses. According to the Solazyme product data sheet, the Soleum™ VHO algae oil we used contained at least 88% oleic acid substituents.<sup>10</sup> In using Soleum™

VHO algae oil we hoped to decrease the MW distribution of our polyol by maximizing the percentage of TG that was monodisperse and able to be functionalized. Although the oil's polydispersity was not able to be tested directly using the common technique of gel permeation chromatography (GPC), precise knowledge of the most abundant fatty acids assisted in the identification of multi-chain glyceride-based polyols using HRMS, which, in turn, allowed for indirect polydispersity estimation (see *Ultra-High-Resolution MS* section below).

In addition to testing algae oil, we also hope to perform GCMS analyses on all polyol products to assess reaction extent and to identify more obscure by-products difficult to distinguish solely on their empirical formulas extracted from HRMS data.

Acid-catalyzed transesterification of algae oil occurred at the glycerol backbone, forming three fatty acid methyl esters (FAME) and one glycerol for each molecule of oil. Silylation converted any alcohol groups present to trialkylsilyl derivatives, allowing them to be volatilized more easily for GC separation. Results for the algae oil GCMS analysis can be seen in Figure 2.3.

GC analysis of the algae oil FAMEs totaled 83.45% by combining the relative percentages of the oleic and monooleoylglycerol derivatives, identifying 95% of oleic components compared to the Solazyme data sheet.<sup>10</sup> Other unsaturated components, 11-eicosenoic acid, and 9-hexadecenoic acid, totaled a mere 1.29% of the total FA content. This allowed for a more accurate interpretation of HRMS peaks, as the high oleic content and low percentage of other unsaturated FA noticeable via GCMS confirmed that the guaranteed percentage of triolein, a monodisperse TG consisting of three oleic acid chains, was least 11% of the total TG content.

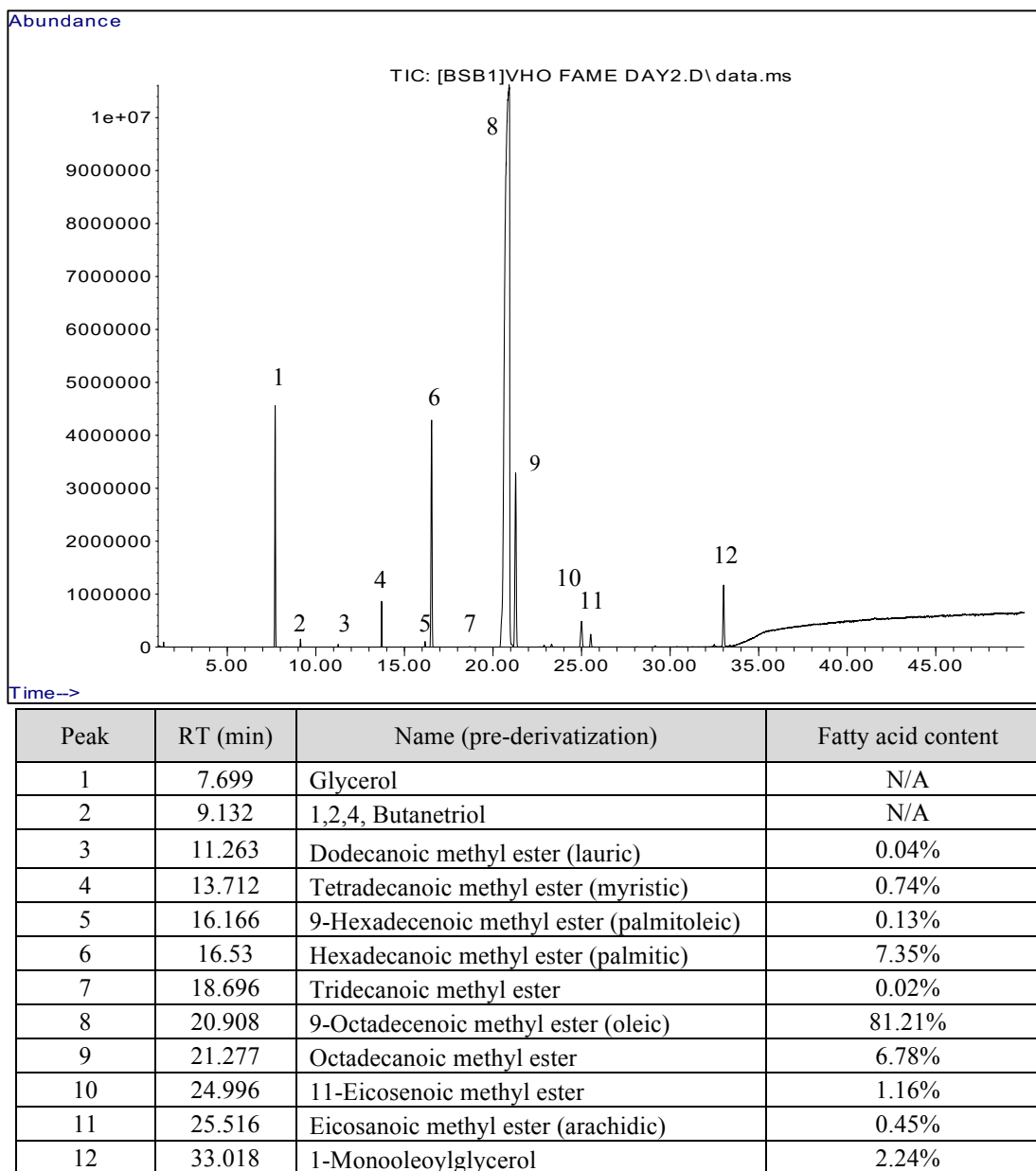


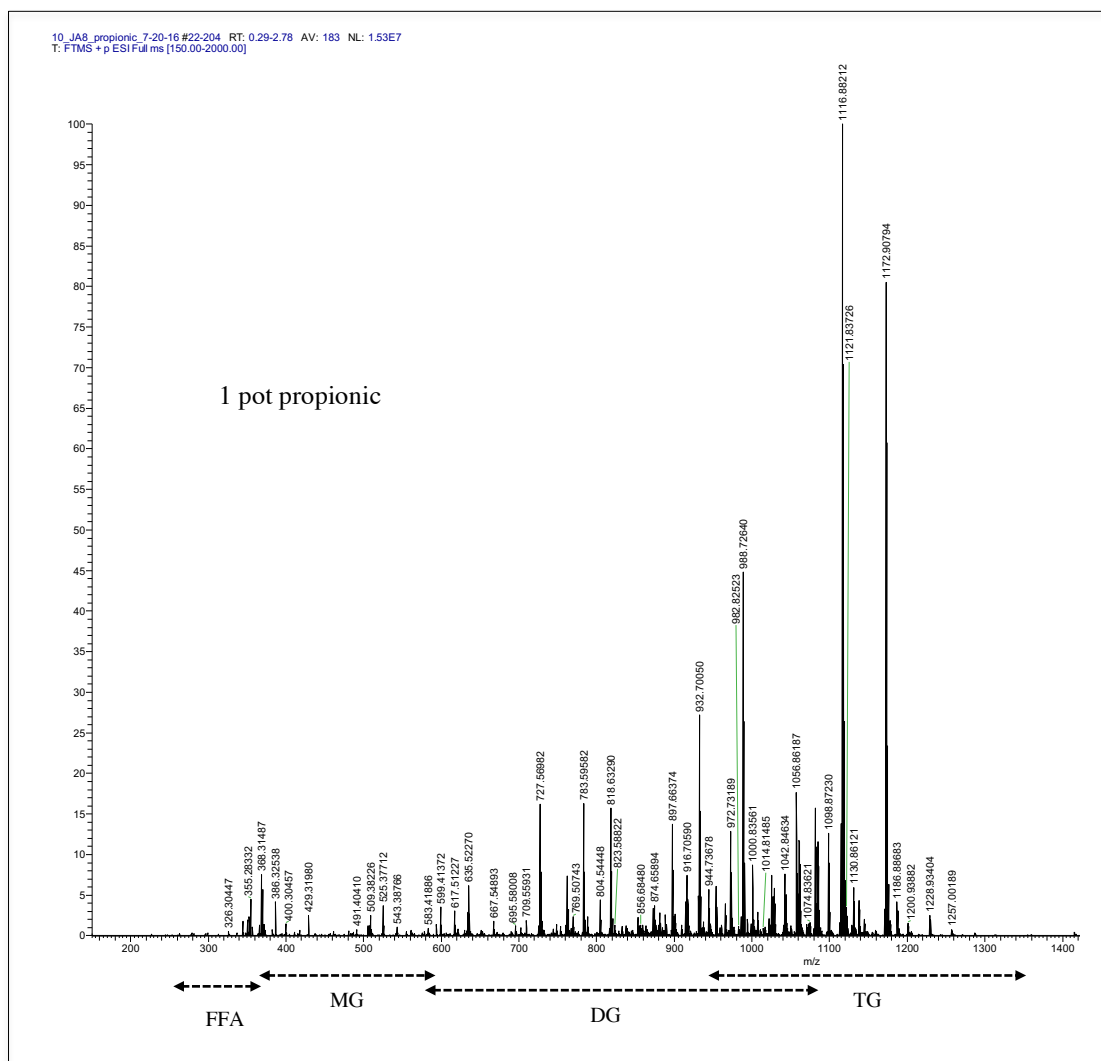
Figure 2.3: Algae oil FAME GC chromatogram and peak table.

### Ultra-High-Resolution MS

The propionic polyol HRMS spectrum was analyzed to approximate the concentrations of each possible substituent attached to the fatty acid chains. HRMS of the 1-pot propionic acid polyol, seen in Figure 2.4, shows that the four major products

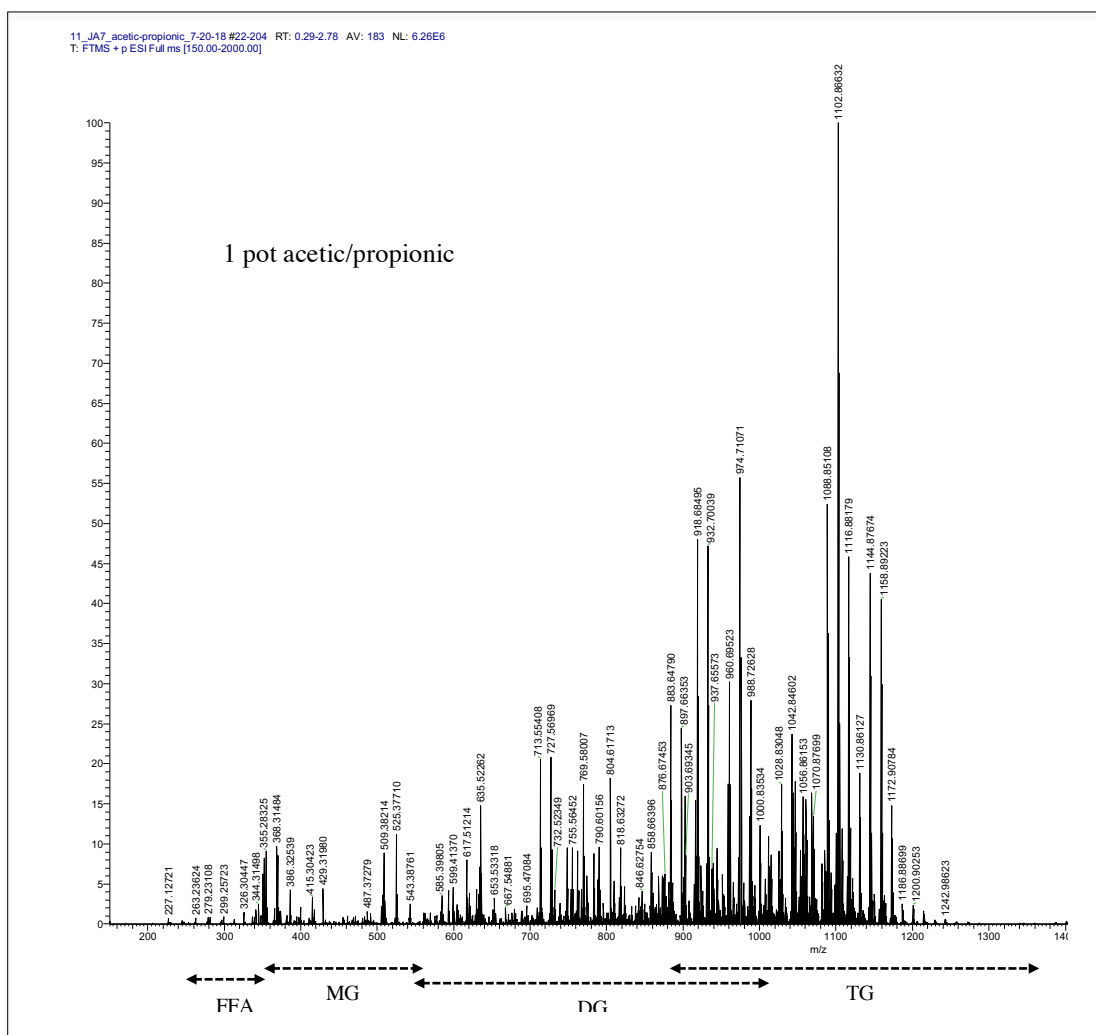
formed were triolein-based polyols, bringing the total triolein content in Soleum™ VHO oil to 27.8% and more than doubling the GCMS-based 11% triolein estimate (see *GCMS* section above). The four triolein-based polyols with relative abundances of 100%, 80.97%, 45.11%, and 12.05% contained the following substituents (in order of decreasing polyol abundance): two propionic and one dihydroxyl substituent ( $m/z = 1116.88212$  Da), three propionic substituents ( $m/z = 1172.90794$  Da), three dihydroxyl substituents ( $m/z = 988.72640$  Da), and one propionic and two dihydroxyl substituents ( $m/z = 1060.85685$  Da). Note that the peak with an  $m/z$  ratio of 932.7005 Da has the third largest abundance at 27.22%, but has not yet been successfully identified. If this compound is classified as a triolein-based polyol, the total monodisperse oleic TG in the original oil sample would be increased to 31%, almost one-third of the overall content.

The presence of significant dihydroxyl substituents, 36% of the four largest peaks, suggests that the rate of acid-catalyzed nucleophilic addition of water was comparable to ring-opening with propionic acid. While the addition of water may be seen as a benefit when higher hydroxyl numbers and greater functionality are required, in this system it contributed to greater MW dispersion by adding unwanted diversity to the oleic polyol substituents and potentially causing hydrolysis of TG ester linkages. Water entered the system within the 30% hydrogen peroxide solution and can theoretically be easily removed using molecular sieves, effectively halting the formation of dihydroxyl substituents.



m/z (Da)	Relative Abundance	TG Chain Identities	Ion
1116.88212	100	PPD	$[M+NH_4]^+$
1172.90794	80.97	PPP	$[M+NH_4]^+$
988.72640	45.11	DDD	$[M+H]^+$
932.70050	27.22	=3 x dihydroxyl oleic – 56.026	?
1060.85685	12.05	PDD	$[M+NH_4]^+$

Figure 2.4: HRMS of propionic acid polyol and identification of a select group of peaks. P=oleic acid with propionic substituent, D=oleic acid with dihydroxyl substituents. Approximate ranges of glycerides with decreasing chains have also been illustrated.



m/z	Relative Abundance	TG chain identities	Ion
1102.86632	100	PAD	$[M+NH_4]^+$
974.71071	55.92	=DDD-CH <sub>2</sub>	?
1088.85108	52.86	AAD	$[M+NH_4]^+$
1116.88212	46.79	PPD	$[M+NH_4]^+$
1172.90794	14.78	PPP	$[M+NH_4]^+$
988.72640	27.97	DDD	$[M+H]^+$
932.70050	47.42	DDD - 56.026	?
1060.85685	15.65	PDD	$[M+NH_4]^+$

Figure 2.5: HRMS of 1 pot acetic/propionic acid polyol and identification of a select group of peaks. P=oleic acid with a propionic substituent, D=oleic acid with dihydroxyl substituents, and A=oleic acid with an acetic acid substituent. Approximate ranges of glycerides with decreasing chains have been illustrated.

Additionally, the relative ratios of triglycerides (TG), diglycerides (DG), monoglycerides (MG), and free fatty acids (FA) were compared in each polyol, as TG decomposition during polyol synthesis would increase MW distribution of the final product. Approximate  $m/z$  values of the above glyceride classes ranged between 800-1200 Da, 400-900 Da, 250-400 Da, and 100-400 Da, respectively. As the four largest peaks were located within the TG range, most of the TG were preserved and little transesterification occurred to break the fatty acids from the glycerol backbone. It also indicates that the epoxidation step was not a limiting factor, as most of the oleic double bonds were functionalized.

The addition of acetic acid to the propionic acid synthesis under the same conditions produced markedly different compounds. All major peaks present in the 1-pot propionic reaction were also present in the 1-pot propionic/acetic, but at different relative abundances. The DDD, PPD, and PPP TG abundances decreased by a factor of 1.6, 2, and 5.5, while the 1 x propionic TG increased by a factor of 1.3. A single peak at  $m/z = 1102.86632$  pointed to a large abundance of triolein TG with propionic, acetic and dihydroxyl substituents on each chain. Another peak at 1088.85108 Da with a relative abundance of 52.86% was identified as an AAD TG. Clearly, acetic acid competed with propionic acid during epoxide ring-opening.

## 2.5 Conclusion

Among aliphatic carboxylic acids, it was discovered that the formation of an algal oil polyol through in-situ Prilezhaev epoxidation and ring opening was driven

kinetically by pKa and chain length. The exception was lactic acid, in which the presence of an alpha-hydroxyl group prevented epoxidation. However, it was found that adding acetic acid to the lactic acid reaction, as well as those reactions involving carboxylic acids with higher pKa's, both increased the rate of polyol synthesis dihydroxyl substituent formation and resulted in the significant use of acetic acid as a ring opener. Further research can be done using 3-hydroxypropanoic acid to test the effect of a hydroxy substituent on epoxide formation. Water removal techniques and reaction temperature gradients can also be examined to quench acetic acid ring-opening in dual-acid 1-pot reactions and to control the formation of dihydroxyl substituents. Little TG chain removal was seen in either the 1-pot propionic or the 1-pot propionic/acetic HRMS spectra, suggesting that, under proper control, these reactions can produce polyols with a narrow MW distribution.

## **2.6 Acknowledgements**

Many thanks to Dr. Burkart for his advice and expertise, Rich Cochran for running the HRMS samples, and Jack Lee for his countless hours making and testing polyols.

Chapter 2, in full, is a reprint of material being prepared for publication. Tessman, Marissa; Lee, Yi-Che; Hartel, Nicolas; Talan, Griffin; Bonilla, Brandon; Ramos, Joshua; Burkart, Michael D.; Pomeroy, Robert. 2016. The thesis author was the primary investigator and author of this paper.

## 2.7 References

1. Pfister, D. P., Xia, Y. & Larock, R. C. (2011), Recent Advances in Vegetable Oil-Based Polyurethanes. *ChemSusChem*, 4, 703–717.
2. Ionescu, M. (2005). *Chemistry and Technology of Polyols for Polyurethanes*. Shawbury, Shrewbury, Shropshire, United Kingdom: Rapra Technology.
3. Howard, G. T. (2012). Polyurethane Degredation. In Singh, S. N. Editor (Eds.), *Microbial Degradation of Xenobiotics*, (371-394). Berlin Heidelberg: Springer-Verlag.
4. Monteavaro, L. L., da Silva, E. O., & Costa, A. O. (2005). Polyurethane Networks from Formiated Soy Polyols: Synthesis and Mechanical Characterization. *JAOCS*, 82, No. 5, 365-371.
5. Lligadas, G., Ronda, J. C., Galià, M., & Cádiz, V. (2010). Oleic and Undecylenic Acids as Renewable Feedstocks in the Synthesis of Polyols and Polyurethanes. *Polymers*, 2, 440-453.
6. Abdullin, M. I., Basyrov, A. A., Kukovinets, O. S., Glazyrin, A. B., & Khamidullina, G. I. (2013). *Polym. Sci. Ser. B* 55: 349. doi:10.1134/S1560090413060018
7. Kazemizadeh, Ali Reza, & Ramazani, Ali. (2009). Passerini multicomponent reaction of indane-1,2,3-trione: an efficient route for the one-pot synthesis of sterically congested 2,2-disubstituted indane-1,3-dione derivatives. *Journal of the Brazilian Chemical Society*, 20(2), 309-312. <https://dx.doi.org/10.1590/S0103-50532009000200016>
8. Miao, S., Zhang, S., Su, Z. & Wang, P. (2010), A novel vegetable oil–lactate hybrid monomer for synthesis of high- $T_g$  polyurethanes. *J. Polym. Sci. A Polym. Chem.*, 48: 243–250. doi:10.1002/pola.23759
9. ASTM D7487-13e1, 2013, “Standard Practice for Polyurethane Raw Materials: Polyurethane Foam Cup Test,” ASTM International, West Conshohocken, PA, 2013, DOI: 10.1520/D7487-13E01, [www.astm.org](http://www.astm.org).
10. Soluem High Oleic Oils (2016, May 15). Product Data Sheet from Solazyme. Document Number: C-Q-00245-S01. [www.solazyme.com](http://www.solazyme.com).

## Chapter 3: Rigid Polyurethane Foam from Sustainable Polyols

### 3.1 Abstract

If renewable materials are to be a competitive replacement for petroleum-based compounds, they must perform equally, if not better than their counterparts. Here, we demonstrate the development of rigid polyurethane foam from algae and soy-based polyols, with the goal of the renewable foam having performance characteristics to that of a surfboard blank. We collaborated with Arctic Foam, a local surfboard blank manufacturer. Using Arctic Foam's formula as a benchmark, we tested new formulations including algae oil-based polyols developed in our lab, glycerol, and soy oil-based polyols on both experimental and factory scales. Each sample was measured for density, hardness, and cell size to quantitate the foams' performance characteristics and to relate the macroscopic properties to either process or formula differences. The experimental-scale mold proved decent for identifying large changes in formula, but did not produce comparable foam due to processing differences. The factory test, performed by replacing 36% of the polyols in Arctic Foam's factory formula with soy polyols, showed promising results. Although the foam's hardness was 8 units below the benchmark, we hypothesize this was mostly due to parts of the benchmark formulation that were incompatible with the bio-based polyol, and not due to the polyol itself.

### 3.2 Introduction

Most surfboards are made from a polyurethane core and coated with epoxy resin, both of which are derived from petrochemicals. Advances in green polymer chemistry show that polyurethane can be developed from biological sources.<sup>1</sup> Algae in particular, provides a renewable and sustainable source of oil, from which polyols, one of the major components of polyurethane, can be synthesized (see Ch. 2). Algae produces about 1850 gallons of oil per acre per year, compared to the 48 and 635 gallons per acre/year that crops such as soy and rapeseed (canola) provide.<sup>2</sup> In addition, it can be grown on non-arable land, so it does not need to compete with food production. Algae is a promising source of renewable and sustainable compounds, and improvements in culture maintenance and processing are being actively studied by several companies, such as Sapphire Energy and Solix, and universities, including UCSD's California Center for Algae Biotechnology (cal-CAB).<sup>3</sup> Sapphire energy cultivates a 300 acre algal pond in New Mexico, and Solix produces and processes algae in bio-reactors in Colorado.<sup>4</sup> Despite its numerous advantages, algae technology remains a smaller source of materials, and more expensive than petroleum. To emerge as a successful, competitive material, algae oil must first gain appeal among a market willing to pay a premium for sustainable goods, such as the surfing industry.

Using of algae oil in performance surfboards appeals to the surfing culture. Surfers are uncomfortable with the fact that although they participate in an environmental sport, they use petroleum-based materials with little biodegradability. Algae oil is currently more expensive, but most of the cost of performance surfboards

come from manufacturing, so the overall price increase of an algae-based surfboard would not be significant. This makes the surfboard industry the perfect market to introduce sustainable products.

Previous research has shown that vegetable-oil based rigid foams tend to be softer than petroleum-based foams when used in similar formulas because their polyols' long hydrocarbon chains are highly flexible and do not offer any secondary bonding interactions.<sup>1,5</sup> This presents a potential problem for bio-based polyols' use in a performance surfboard, where core flexibility, durability, and compressive strength carry huge significance. However, many of these studies simply use the same formula, but replace petroleum polyols with bio-based polyols with similar molecular weights, functionalities, and hydroxyl numbers.<sup>6</sup> Here, we seek to develop a workable formula that achieves the mechanical properties of a performance surfboard while increasing the percent renewability as much as possible.

### **3.3 Experimental**

The process for pouring foam included mold preparation, prepolymer preparation, foam pouring, and measurements. We collaborated with Arctic Foam, a surfboard blank manufacturer located in Oceanside, California to produce four types of foams using two scales to compare small-scale, in-lab tests with full-scale surfboard production. The four tests were the following: a small-scale control using Arctic Foam's formula, a small-scale test in which 28% of the polyols were the algae-based lactic acid polyol described in Chapter 2, an Arctic Foam surfboard blank as a full-

scale control, and a full-scale surfboard using the same Arctic Foam formulation, but exchanging 36% of the polyols with soy-derived polyol from MCPU Engineering. The final test was performed with the idea that MCPU would be able to produce polyols from algae oil comparable to their soy polyols. The processing steps are detailed in the following sections for the small-scale mold only. The procedures and formulations surrounding the large-scale blank preparation are the intellectual property of Arctic Foam, and cannot be disclosed here.

### 3.3.1 Pipe Mold Preparation

Parchment paper was rolled approximately four layers thick and slid into the pipe mold so that about 2 cm protruded from either side. Four slits were cut into the excess paper and folded outwards. One side of the mold was covered with another piece of parchment paper, followed by a wood block and secured by a zip tie. Paper and wood were used to cover the other side of the pipe and were secured by a C-clamp. Prior to use, the mold was preheated in an oven set at 43 °C for at least 10 mins. The completed mold setup can be seen in Figure 3.1, and materials are listed in Table 3.1.



Figure 3.1: Mold Setup

Table 3.1: Materials and chemicals for rigid polyurethane. Polyols A, B, C, and J are the intellectual property of Arctic Foam.

Pipe Mold	Chemicals	Miscellaneous
Metal pipe 10.2 cm length, 5.3 cm ID	Polyols: A, B, C, J, trimethylol propane (TMP), glycerol	Drill press and stirring bit
Parchment paper	Blowing Agent: distilled water	IR temperature gun
Zip tie, 24 in (or 3 x 11 in.)	Catalyst/silicone mixture: F	Fridge set to 15 °C
Two 3 ½ x 3 ½ x ¾ inch square wood blocks	Diisocyanate: 2, 4-toluene diisocyanate (TDI)	Oven set to 43 °C
C-clamp with at least a 16 cm span		Respirator
		Durometer Type O (ASTM 2240)

### 3.3.2 Prepolymer Preparation

TMP was melted on a hot plate (mp: 58 °C). To a pre-weighed cup, the appropriate weights of components A, B, C, J, DI, and TMP or glycerol were added, being careful to avoid smearing or splashing components on the side of the cup as this would prevent homogeneous mixing. The components were thoroughly mixed at 2900 rpm using a paint mixer attached to a drill press and reweighed to determine the weight of components lost during mixing. Using that weight, the amount of TDI needed for the required iso-index was calculated. The cup was transferred to a fridge set at 15 °C and let sit until thermal equilibrium.

### **3.3.3 Foam Pouring**

Before taking the pre-polymer out of the fridge, the mold, pre-heated at 43 °C, was removed from the oven. The appropriate amounts of components F and TDI were added. Using the drill press and paint stirrer, the polymer/TDI was mixed and monitored with an infrared temperature gun until the temperature reached 22-23 °C. Once the target mass had been added to the tared mold, the mold was quickly closed and placed in the oven for 25 mins, after which the foam was removed from the mold and placed in a slightly humid oven set at 60 °C for 2.5 hours.

### **3.3.4 Measuring Density and Hardness**

The Arctic Foam surfboard, control, and renewable foam cores were cut into slices approximately 0.6 to 1.0 cm long. The densities were measured using the core slice dimensions divided by their mass. The hardness of each core slice was measured in several different places using a Type O Durometer (ASTM D2240),<sup>7</sup> and the measurements were averaged.

## **3.4 Results and Discussion**

While the PU formulas can be scaled up from experimental to production sizes with only slight changes, their processing methods must be substantially modified, which impacts the physical properties of the foam. Important inconsistencies between the small-scale pipe molds and full-scale surfboard molds were noted by comparing densities and hardness throughout their core samples (Figure 3.2). The densities of

both the full-scale Arctic Foam and 36% soy surfboards decreased predictably towards the center of their cores, consistent with a mold under partial pressure. Their overall densities were  $44 \pm 12$  g/L and  $40 \pm 12$  g/L, respectively, including the denser outer edges (not included in Figures 3.2 and 3.3), and  $41 \pm 3$  g/L and  $37 \pm 4$  g/L, respectively, after removing the edges from the data set.

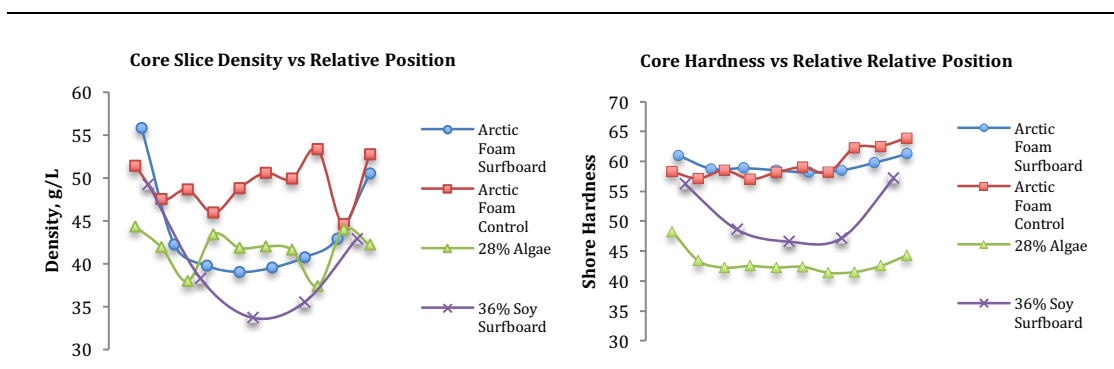


Figure 3.2: Core slice densities and hardness relative to position in the core.

On the other hand, the density of the Arctic Foam control,  $49 \pm 7$  g/L, surpassed that of the large-scale Arctic Foam surfboard,  $41 \pm 3$  g/L, and the uncertainty increased by a factor of 2.3 due to random density fluctuations throughout the core. Both the higher density and uncertainty in the small-scale Arctic Foam control occurred because of processing differences. More solid material per unit volume stayed in the small-scale mold either because more material was added initially, or because the small-scale mold was more pressurized than the large-scale mold, allowing less material to expand through the gaps in the top and bottom. Despite differences in density, the mold produced an Arctic Foam control with a hardness identical to the surfboard, though again more inconsistent, at  $59 \pm 7$  compared to  $59 \pm$

2. Deviations between scales meant that it was impossible to apply small-scale results to the factory scale. Small-scale tests could be performed initially, but large-scale tests must ultimately determine performance.

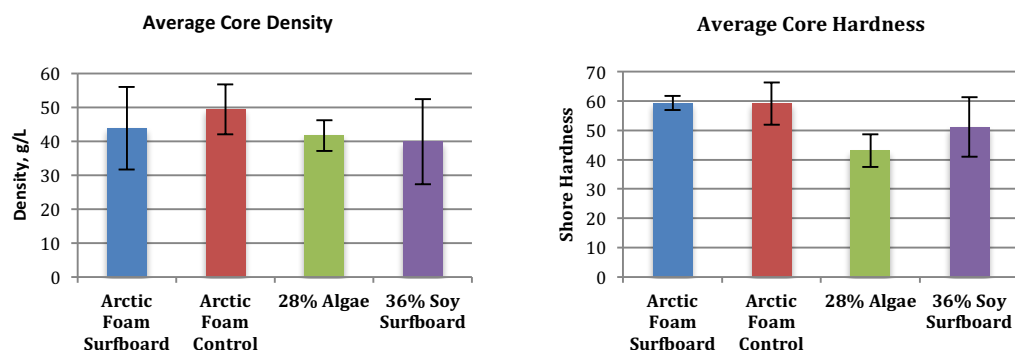


Figure 3.3: Average core density and hardness of four rigid foam samples

Inconsistencies between the industry mold and the experimental small-scale mold were also evident in the characteristics of the PU cells. As seen in Figure 3.4 (top left), the cells in the full-scale Arctic Foam mold were round and similarly-sized with thin, even struts, whereas the cells from the small-scale control mold (Figure 3.4, top right) varied in size, shape, and strut thickness. Cells form and burst according to the kinetics of gas formation and the fluid dynamics that govern how material drains from the cell walls. Temperature, mix time, and mold pressure play a role in reaction speed, gas pressure, and cell wall surface tension.<sup>8</sup> Surfactant concentration also contributes to cell formation and opening, but as the formula was kept constant between the large-scale Arctic Foam surfboard and small-scale Arctic Foam control, it can be assumed that process differences were the only factor. The 36% soy surfboard blank made at full-scale (bottom right) demonstrated similar rounded, defined cells

compared to the full-scale control despite having formula differences, a trait not seen in either small-scale tests. This further supported the hypothesis that some cell features were a function of process.

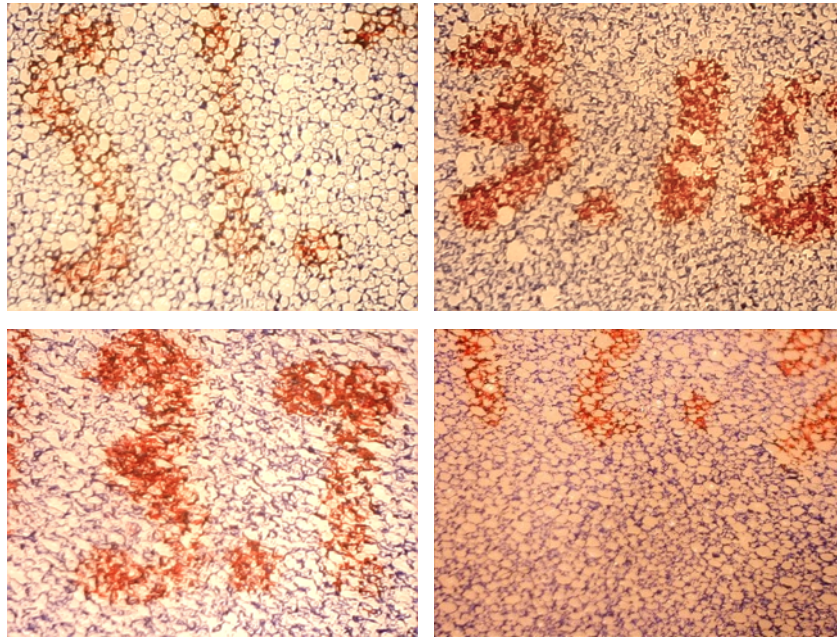


Figure 3.4: Images of cells in representative core slices: surfboard (top left), control (top right), 28% algae (bottom left), and 36% soy surfboard (bottom right). The core slices were colored with blue ink before being photographed under a microscope at 10x scale.

Although the process differences between scales prevented small formula changes from being detected with any accuracy, larger changes were noticeable. As the goal was to produce a full-scale surfboard, the test directly replacing 36% of Arctic Foam's polyol with soy polyol provided interesting insight into formulation changes. The soy board was slightly less dense than the full-scale control, indicating that less solid mass was added to the mold. It also may have indicated that although equal masses were added in both tests, more material expanded beyond the mold due to the

addition of too much blowing agent, a behavior expected, but controlled in the full-scale, partially-pressurized molds. The mass of over-expansion was not recorded in this test, so the validity of this hypothesis cannot be confirmed, however, the 36% soy core's hardness also indicated that the foam expanded too much. While the control board's hardness remained relatively constant throughout the entire length of the core sample (excluding the tough outer edges), the 36% soy's hardness decreased towards the center relative to its decrease in density. By decreasing the amount of blowing agent and catalyst cocktail (F), or the ratio of blow to gel catalyst, it is possible that a harder board with comparable density can be created.

Conversely, the surfactant type or concentration may have played a role in the hardness decrease. The surfactant used in the small-scale 28% algae and full-scale 36% soy formulas was the same used in the Arctic Foam formula. Surfactants reduce bubble surface tension, which allows the cells to open more easily, and causes gases produced by the blowing agent to aggregate in larger bubbles. The cell sizes apparent in the bottom right panel of Figure 3.4 are smaller and with a larger size distribution, and the struts between the cells were thicker and more clumped compared to the control (top left). Either too little or the wrong kind of surfactant would prevent the cell wall material from draining properly, which would explain both the lack of bubble aggregation and the thick struts. Surfactants are chosen based on their ability to interact with either polyethers or polyesters. Because the surfactant used here was designed to be used in a polyether polyol matrix, it is likely that it would react differently in polyether/polyester hybrid. Several additional full-scale tests were

performed that verify the water/catalyst hypothesis, but core samples could not be obtained for analysis as Arctic Foam deemed the qualitative characteristics acceptable for a prototype and produced finished surfboards from them. Surfactant tests have not yet been performed.

Reformulating the control and substituting 28% of the polyol components with algae-based polyols in the small-scale test, resulted in a substantial decrease in hardness ( $43 \pm 6$ , 16 units lower than the control) and a slight decrease in density ( $42 \pm 5$  g/L, 7 g/L lower than the control). While a lower density can be explained by having less material in the mold, the hardness level was too low to be explained only by a proportional decrease in density. In comparison, the hardness measurements between the small-scale control and full-scale surfboard remained constant despite density differences, most likely due to petrochemical polyethers having more uniform hydrogen bonds than the bio-based polyesters in PUs, leading to the conclusion that the 28% algae formulation produced softer foam. Additionally, the cells in the 28% algae foam did not have well-defined struts, circular shapes, or uniform sizes (Figure 3.4 bottom left). While this can be at least partially explained by small-scale mold processing, the degree of cell-openness and amorphous shape cannot be explained by process alone (compare to small-scale control, Figure 3.4 top right). It is possible that the amount of blowing agent, surfactant, or catalyst caused the cells to burst before their walls had begun to set, leading to over-nucleation of the escaping gases. This would explain the uneven and amorphous cells. Further testing would need to be done to eliminate these variables as the sole cause of the foam's lack of hardness by

measuring cream time, tack free time, free-rise temperatures and heights as a function of time,<sup>9</sup> in addition to hardness, density, and cell size.

Until a full spectrum of formulas have been tested at factory scale, no quantitative conclusion can be reached as to the quality of either renewable formula. However, a number of MCPU's "Honey Bee" polyol features can be examined to determine its quality in the 36% bio-based foam. First, the formula replaced a polyether polyol that had a hydroxyl number of around 550 mg KOH/g with a 50:50 mix of polyester polyols having hydroxyl numbers of 530 and 230 mg KOH/g, giving the new mix an average hydroxyl number of 380 mg KOH/g, almost a 200 mg KOH/g decrease. As stated in Chapter 1, hydroxyl number is directly proportional to hardness, so an overall decrease would produce softer foam.

Honey Bee polyols are synthesized in a process similar to the one described in Chapter 2, in which hydroxyl groups are added to the double bonds in fatty acid chains, and the triglycerides remain largely intact.<sup>10</sup> Regardless of the hydroxyl number, the renewable polyols are branched at the glycerol backbone, which gives the soft domain less flexibility. The presence of the three polar esters on the glycerol backbone also enables hydrogen bonding with the amine in the urethane hard segments. The result of both characteristics produce a quasi-hard segment in the center of each polyol which increases mixing between the soft and hard segments, preventing the formation of large, crystalline hard segments that contributes to macroscopic rigidity. They also contain "dangling chains", or the 9-18 carbon chains originating either from a saturated fatty acid chain present in about 15% of the soy oil, or from the

tail end of a functionalized fatty acid. As previous research has discovered,<sup>1,4</sup> these dangling chains can increase flexibility and reduce rigidity due to their amorphous nature within the soft segments.

However, although the Honey Bee 230 has a functionality of 2, identical to the polyether polyol, the Honey Bee 530 has a functionality of 6, meaning that all three of its fatty acid chains are di-functionalized. Because the hydroxyl groups are in close proximity, a higher functionality would naturally produce a larger hard segment less affected by soft segment compatibility. By utilizing Honey Bee 530 in the formula, it is possible that the softness produced by using oil-based polyols can be remedied.

### **3.5 Conclusion**

Small-scale molds can be used to track large formula changes, however, most testing should be performed at the intended scale due to processing differences. The bio-based polyols followed previous research, producing foams softer than their petroleum-based counterparts. Their softness, however, may be due to formulation variables independent of the polyol itself, such as surfactant, blowing agent, and catalyst, and can be helped by the addition of high functionality polyols.

### **3.6 Acknowledgements**

Thank you to Arctic Foam for partnering with our lab and enabling us to experiment with your materials, formulation, and facilities. I would also like to

acknowledge the many workers and volunteers who helped with this project including, but not limited to Trevor Anderberg, Griffin Talan, Yi-Che (Jack) Lee, Stephen Lo, Daniel Pham, and Chris Mayfield, as well as Wendy Groves and Heidi Trimble. Thank you to the UCSD Chemistry and Biochemistry Department for allowing us to use their facilities, and to Skip Pomeroy and Steve Mayfield for allowing us space in their labs.

### 3.7 References

1. Meier, M., Metzger, J., & Schubert, U. (2007). Plant oil renewable resources as green alternatives in polymer science. *Chemical Society Reviews* 36.11: 1788-1802.
2. Riesing, T. F. (2005). Cultivating algae for liquid fuel production. *Global Energy Network Institute*. Retrieved from: <http://www.geni.org/globalenergy/library/technical-articles/generation/future-fuels/permacultureactivist/cultivating-algae-for-liquid-fuel-production/index.shtml>
3. Haro, A. (2015, April 25). World's First Algae-Based Surfboard Made by Chemistry Students. *The Inertia*. Retrieved from: <http://www.theinertia.com/surf/worlds-first-algae-based-surfboard-made-by-chemistry-students/>
4. Jacquot, J. (2009, October 12). 5 Companies Making Fuel From Algae Now. *Popular Mechanics*. Retrieved from: <http://www.popularmechanics.com/science/energy/a4677/4333722/>
5. Velayutham, T. S., Majid, W.H., Ahmad, A.B., Gan, Y. K., & Gan, S. N. (2009). The physical and mechanical properties of polyurethanes from oleic acid polyols. *J. Appl. Polym. Sci.* 112 (6), 3554-3559.
6. Madden, J. P., Baker, G. K., and Smith, C. H. (1971). *A study of polyether-polyol- and polyester-polyol-based rigid urethane foam systems*. No. BDX--613-531; CONF-710913--1. Allied-Signal Aerospace Co., Kansas City, MO (United States). Kansas City Div.

7. ASTM D2240-00, 2000, “Standard Practice for Rubber Property-Durometer Hardness,” ASTM International, West Conshohocken, PA, 2000, DOI: 10.1520/D2240-00, [www.astm.org](http://www.astm.org).
8. Kaushiva, B. D. (1999). *Structure-Property Relationship of Flexible Polyurethane Foams* (Doctoral Dissertation). Retrieved from: <https://theses.lib.vt.edu/theses/available/etd-083199-185156/unrestricted/KAUSHIVA1.PDF>
9. ASTM D7487-13e1, 2013, “Standard Practice for Polyurethane Raw Materials: Polyurethane Foam Cup Test,” ASTM International, West Conshohocken, PA, 2013, DOI: 10.1520/D7487-13E01, [www.astm.org](http://www.astm.org).
10. Garrett, T. M., and Du, X. X. Honey Bee: Polyols for Diverse Applications. MCPU Engineering.

## **Chapter 4: Eco Friendly Quality Analysis: A Greener Method for Measuring Polyol Hydroxyl Number Using FTIR-ATR Spectroscopy**

### **4.1 Abstract**

A new method for the determination of polyol hydroxyl number using Fourier Transform Infrared-Attenuated Total Reflectance (FTIR-ATR) spectroscopy was developed. Two independently synthesized series of soy-based polyols with known hydroxyl numbers were scanned directly on an FTIR-ATR spectrometer. Certain characteristic peaks were shown to increase linearly with hydroxyl number for each series, producing calibration curves with correlation constants of 0.9944 and 0.9998, and median uncertainties of 5.6% and 3%. As the current methods are slow, toxic, and expensive, this method presents a greener, cheaper alternative that can help plant-based polyols compete with those synthesized from petroleum.

### **4.2 Introduction**

Polyols are polyether, polyester, or hydrocarbon chains consisting of multiple hydroxyl groups. As the precursor to a wide variety of polymers, polyol production plays an essential role in many facets of industry. Because of its widespread use, the polyol manufacturing process is being re-evaluated for potential areas of improvement. In particular, researchers strive to produce more environmentally safe protocols that maintain, if not improve, quality and cost.<sup>1,2</sup> Most polyols are currently created from petroleum, which poses a large barrier to their development as a green

product. As a result, most researchers have focused on developing quality polyols from different sources, particularly vegetable oils. This research has produced some promising results; bio-based polyols are now available at companies such as Emery Oleochemicals, MCPU Engineering, and Cargill.<sup>3,4</sup> Less attention has been given to some of the other aspects of polyol manufacturing. This study explores one possible area of improvement: the method for determining the hydroxyl value of plant-based polyols.

Hydroxyl value (also called hydroxyl number) is important for both quality analysis (QA) and quality control (QC) purposes. During polymerization, polyol hydroxyl groups react with diisocyanate to produce polymer chains and crosslinks. The amount of hydroxyl groups present per gram of polyol influences crosslink formation, which has a direct effect on the physical characteristics of the resulting polymer.<sup>5</sup> Hydroxyl value can also be used in process to test polymerization completeness.<sup>6</sup>

Standard determination methods involve acetylation (ASTM D4274 and E222) or carbamate formation and subsequent titration (ASTM E1899), with variations to account for different acidities and chemical makeup. These methods are time-consuming and rely on large volumes of expensive, toxic chemicals such as pyridine, p-toluenesulfonyl isocyanate, 4-dimethylaminopyridine (DMAP), N

N-methylpyrrolidone (NMP) and acetic anhydride (see Supporting Information section for MSDS References).<sup>7,8,9</sup> In ASTM D4274-05, for example, the acetylation

reaction used to prep each sample for titration takes about 30 minutes to complete, and costs over \$6 in reagents alone (reagent plus blank) according to an analysis of reagent prices.<sup>10</sup> Additionally, the disposal of these chemicals as hazardous waste can cost up to ten times the cost of the chemical itself.<sup>11</sup> In the 2014 Wiley Series on Polymer Engineering and Technology, titration methods are cited as having “below average” reliability due to the variety of methods and deviations among operators, advising that manufacturer hydroxyl numbers may vary by as much as 10%, although the titrations are also cited as having a 1% precision in the 95% confidence interval if performed properly.<sup>12</sup> Because plant-based polyols are still an emerging product, the cost, environmental impact, and unreliability of chemical titration methods inhibit their ability to compete with existing petroleum-based polyols.

In an effort to avoid using titration methods, near infrared (NIR) spectroscopic techniques using partial least squares (PLS) software have been developed and are now included as approved ATSM methods (ASTM D6342).<sup>13</sup> These have considerable time and preparatory advantages, as well as reasonable accuracy. NIR spectroscopic methods published by Metrohm and Perkin Elmer were comparable to chemical titration to within 5 mg KOH/g.<sup>14,15</sup> Many companies have not adopted these methods, however, most likely due to the cost of the instrument and accompanying PLS software. NIR spectrometer prices range from \$30,000 to \$35,000, with additionally costs for sample cells. The NIR also takes many samples to create a calibration curve.

Although research into environmentally friendly spectroscopic techniques for measuring hydroxyl number has largely revolved around the NIR, Fourier Transform infrared – attenuated total reflectance (FTIR-ATR) spectroscopy offers a comparable

and practical alternative. Like the NIR, it is quick, inexpensive, and non-destructive. The ATR cell enables viscous polyol samples to be measured directly without any preparation, eliminating all of the reagent costs associated with the titration methods. FTIR-ATR spectrometers display higher intensities than their NIR counterparts, and are already heavily used in industrial settings for the characterization of polyols. FTIR-ATR spectrometers are less expensive than NIRs, costing around \$25,000. These qualities give the FTIR-ATR the potential to become a valuable, multifaceted instrument for polyol analysis.

The difficulty in using the FTIR for many types of quantitative analysis lies with the construction of a calibration curve that can be applied to a wide variety of samples. Each sample in question has a unique spectrum, and while that makes the FTIR a popular instrument for identification, its applications elsewhere have been limited. This behavior can be seen among polyols. Polyols produce spectra that are too diverse due to varying starting materials and syntheses. Not only are polyols divided into polyether and polyester categories, they can be synthesized from many different oils (e.g. petroleum, soy, algae). Even amongst polyols with the same source, the methods for synthesis are just as varied. Some of the most common methods include iodination and substitution with alcohol-containing compounds, and epoxidation followed by ring opening.<sup>16,17,18</sup> This means that polyols developed from identical oils can have different spectra as well.

The natural peaks to use for quantitation would be those that all polyols have in common: the OH peak around  $3400\text{ cm}^{-1}$  and the CH stretches around  $2900\text{ cm}^{-1}$ . However, these peaks also change depending on structure. Differing molar

absorptivities,  $\lambda$  maxes, and peak ratios can occur due to varying degrees of hydrogen bonding, peak overlap from bonds with similar resonance frequencies, and the type of synthesis taking place. Because of these factors, any calibration must be source and synthesis-specific. In this study, calibration curves for two soy-based polyols created from different processes have been constructed to demonstrate that although a universal calibration curve cannot be made, individual curves based on source and synthesis have comparable accuracy to those of the titrations and NIR.

### **4.3 Experimental**

Biobased Technologies® contributed four standards with hydroxyl values of 70, 110, 134, 159 mg KOH/g from their line of Agrol® polyols made from soybean oil as well. MCPU Engineering donated five soy-based Honey Bee™ Polyol standards with hydroxyl values of 56, 57, 150, 230, and 530 mg KOH/g. A drop of each polyol standard was scanned directly on a Perkin Elmer Spectrum RX FTIR spectrometer using a Pike Tech 1 mm ZnSe ATR cell. 25 scans were taken at a 2.0  $\text{cm}^{-1}$  resolution over a range of 4000 to 600  $\text{cm}^{-1}$ , which took approximately one minute to complete. An atmospheric background was taken before the first standard and applied to all standards. Using Matlab and Excel, the resulting spectra were characterized to evaluate similarities and differences between the two types of polyols, and to determine which peaks could be used for quantitation. The possible peaks were then used to create calibration curves.

## 4.4 Results and Discussion

### 4.4.1 Characterization

The absorption spectra for the Agrol and Honey Bee polyols were plotted in Figure 1. Both plots clearly showed the characteristic polyol peaks as well as peaks unique to their synthetic processes. Characterization aided in the selection of peaks suitable to use for calibration.

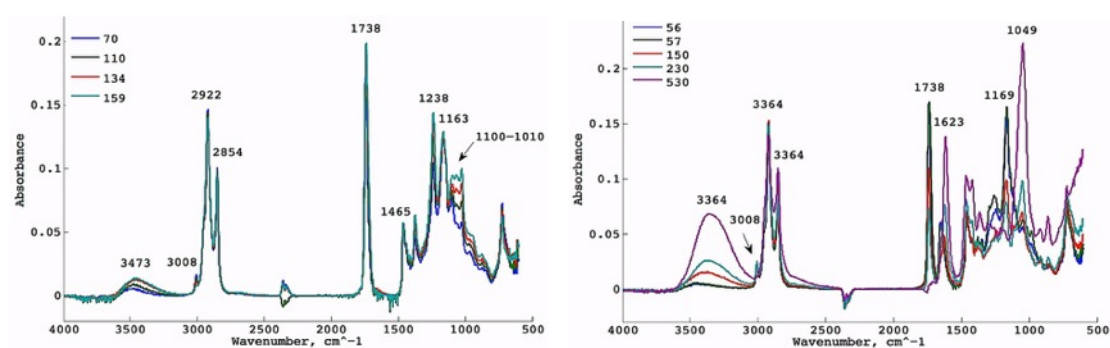


Figure 4.1: FTIR spectra of polyol standards from Agrol and Honey Bee. Each spectrum has been normalized according to the baseline between 2200 and 1900  $\text{cm}^{-1}$ , and is labeled with its respective manufacturer-reported hydroxyl value. Major characteristic peaks have also been labeled for both spectra.

The Agrol samples (Figure 5.1, left) displayed peaks typical of a polyether polyol: an O-H peak located at  $3473 \text{ cm}^{-1}$ , alkane C-H stretches at  $2922$  and  $2854 \text{ cm}^{-1}$ , a C-H bending peak at  $1465 \text{ cm}^{-1}$ , a C=O stretch at  $1738 \text{ cm}^{-1}$  from a terminal ester, and multiple C-O stretches and O-H bends in the fingerprint region. The spectra also included a C=C-H stretch at  $3008 \text{ cm}^{-1}$  that decreased with increasing hydroxyl number, indicating that the synthesis of polyols involved the addition of OH groups through varying degrees of epoxidation and ring opening with alcohol. A closer look at the fingerprint region also revealed the increase in hydroxyl number across the

samples. The C=O stretch at  $1738\text{ cm}^{-1}$  and the C-O-C stretch at  $1163\text{ cm}^{-1}$  remained relatively constant over all standards, indicating that the terminal ester group did not participate in the formation of polyols. On the other hand, the C-O and O-H peaks at  $1238\text{ cm}^{-1}$  and in the  $1178\text{-}985\text{ cm}^{-1}$  range grew significantly due to the increase in ether and alcohol groups present along the chain.

The Honey Bee samples (Figure 5.1, right) had a more complicated spectrum due to a different manufacturing process. Alcohol functional groups were added to unsaturated carboxylic acid chains (derived from the esterification of soybean oil triglycerides) through the addition of an alcohol amine. The alcohol amine also reacted with the carboxylic acid group to form an esteramide. These reactions were apparent in the change in characteristic peaks as a function of hydroxyl number. As more functional groups were added across the double bond, the C=C-H alkene peak at  $3008\text{ cm}^{-1}$  shrank. Formation of an esteramide was shown in the growth of the carbamate peak at  $1623\text{ cm}^{-1}$  and the shrinking of the C=O ester peak at  $1738\text{ cm}^{-1}$ . The C-O-H peak at  $1049\text{ cm}^{-1}$  and the O-H stretching peak within the  $3500\text{-}3100\text{ cm}^{-1}$  range also grew as a function of increasing hydroxyl number.

#### **4.4.2 Calibration**

Calibration curves were developed individually for the Agrol and Honey Bee polyol standards, displayed in Figure 5.2. The characteristic peaks directly related to the addition of OH groups (e.g. the OH stretching or CO-H peaks) displayed the greatest sensitivity with increase in hydroxyl number, and were therefore used for calibration. Additionally, the CH peak with the largest molar absorptivity was

selected as an internal standard for both series of standards. The hydroxyl values used in the calibration were those given by the manufacturers.

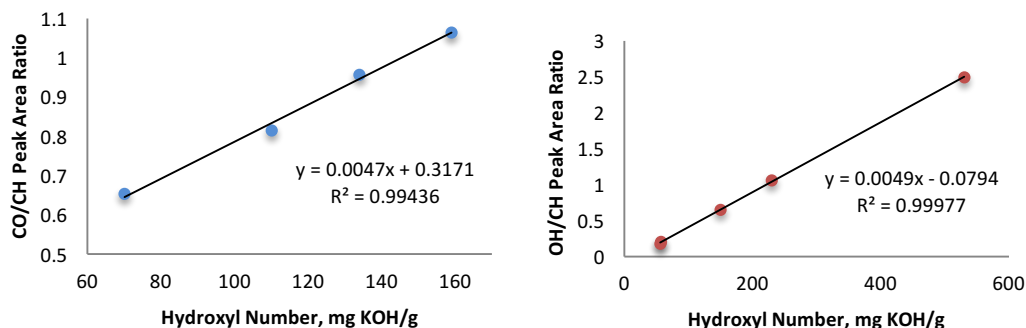


Figure 4.2: Calibration curves for Agrol (left) and Honey Bee (right) polyol standards. For the Agrol standards, CO-H peak areas produced the most accurate calibration, and was calculated between 1330 and 1207  $\text{cm}^{-1}$ . For the Honey Bee standards, the ratio between the OH and CH peaks produced the most accurate calibration. The OH peak area was calculated over the 3600-3050  $\text{cm}^{-1}$  range, and the CH peak area was calculated over the 2980-2880  $\text{cm}^{-1}$  range.

The Agrol polyols absorbed linearly in the OH stretching region of the spectrum, but the peak intensities were not strong enough for a precise calibration curve to be made (a calibration curve of OH/CH peak area ratios produced a correlation coefficient of only 0.9857). Instead, the standards were calibrated using a ratio of the peak area between 1078 and 985  $\text{cm}^{-1}$  and the CH peak area between 2980 and 2880  $\text{cm}^{-1}$ . The calibration curve had a correlation coefficient of 0.9944, and a standard error of the y estimate of 0.016, resulting in a 95% confidence interval of  $\pm 5$  mg KOH/g. The upper and lower ends of the curve displayed uncertainties of 6.6% and 2.9%. The Series 1 curve was tested via a 1:1 mixture of the 110 and 134 polyols that had a calculated hydroxyl number of 122 mg KOH/g. The estimated value was 128 mg KOH/g, 6 mg KOH/g and 5.6% higher than the calculated value.

The Honey Bee calibration curve was based on the ratio of the OH stretch and CH stretch peak areas in the ranges 3600-3050  $\text{cm}^{-1}$  and 2980-2880  $\text{cm}^{-1}$ , respectively. The correlation constant of the curve was 0.9998, suggesting a highly linear trend. The standard error of the y estimate was 0.017, corresponding to an uncertainty of  $\pm 7$  mg KOH/g (95% CL). The upper and lower ends of the curve displayed 1.3% and 12% uncertainties. The median uncertainty was about 3%. Similarly to Agrol, a 1:1 mixture of the 150 and 230 hydroxyl value standards with a calculated hydroxyl value of 191 mg KOH/g was created to test the curve. The value given by the curve was 195 mg KOH/g, falling well within the expected uncertainty range. The 56 and 57 standards' signals were not reproducible, so the creation of a separate calibration curve for smaller hydroxyl values is advised.

#### **4.5 Conclusion**

With a basic spreadsheet program and a few standards, calibration curves were created from FTIR-ATR spectra that gave results remarkably close to existing titration and NIR methods. The method for quantifying hydroxyl number provided here was tested on soy polyols from two kinds of processes as a proof of concept. Further investigation must be done to confirm its application to polyols with different starting materials. However, its simplicity, speed, and accuracy are promising.

#### 4.6 Acknowledgements

I would like to thank MCPU Engineering and Biobased Technologies for their sample donations, Robert Pomeroy for allowing me to use his lab space, and for his guidance on this project, and UCSD's Biochemistry and Chemistry Department.

Chapter 4, in full, is a reprint of material currently submitted for publication. Tessman, Marissa; Burkart, Michael; Pomeroy, Robert. "Eco Friendly Quality Analysis: A Greener Method for Measuring Polyol Hydroxyl Number Using FTIR-ATR Spectroscopy", 2016. The thesis author was the primary investigator and author of this paper.

#### 4.7 References

1. Pfister, D. P., Xia, Y. & Larock, R. C. (2011), Recent Advances in Vegetable Oil-Based Polyurethanes. *ChemSusChem*. 4, 703–717.
2. Campanella, A., Bonnaille, L., Wool, R.P. (2009). Polyurethane Foams From Soyoil-Based Polyols. *J. Appl. Polym. Sci.* 112, 2567-2578.  
<http://onlinelibrary.wiley.com/doi/10.1002/app.29898/full>.
3. Eco-Friendly Polyols Product Overview. (2014).  
<http://www.emeryoleo.com/content/EP%20Product%20Overview.pdf> (accessed July 11, 2015). Emery Oleochemicals.
4. BiOH polyols and polymers. (2015).  
<http://www.cargill.com/company/businesses/biohpolyols/index.jsp> (accessed July 11, 2015). Cargill.
5. Tu, Y. C. (2008). Polyurethane Foams From Novel Soy-Based Polyols (Ph.D Dissertation). University of Missouri, Columbia, MO.
6. *FT-NIR for Online Analysis in Polyol Production*; Application Note 51594 for Thermo Scientific: Madison, WI, 2008.

7. ASTM D4274-11, (2011). *Standard Test Methods for Testing Polyurethane Raw Materials: Determination of Hydroxyl Numbers of Polyols*, West Conshohocken, PA: ASTM International, [www.astm.org](http://www.astm.org).
8. ASTM E222-10, (2010). *Standard Test Methods for Hydroxyl Groups Using Acetic Anhydride Acetylation*, West Conshohocken, PA: ASTM International, [www.astm.org](http://www.astm.org).
9. ASTM E1899-08, (2008). *Standard Test Method for Hydroxyl Groups Using Reaction with p-Toluenesulfonyl Isocyanate (TSI) and Potentiometric Titration with Tetrabutylammonium Hydroxide*, West Conshohocken, PA, ASTM International, [www.astm.org](http://www.astm.org).
10. *Automated determination of the hydroxyl number (HN) according to ASTM E 1899-08 and DIN 53240-2*; Application Bulletin No. 322 e For Metrohm: Riverview, FL.
11. Hazardous Waste Determination and Classification Guideline, (2013). *UC Santa Cruz Environmental Health and Safety*. <http://ehs.ucsc.edu/programs/waste-management/documents/hw-guide1.pdf> (accessed July 11, 2015).
12. Sonnenschein, M. (2015) Theoretical Concepts and Techniques in Polyurethane Science. *Polyurethanes: Science, Technology, Markets, and Trends* (127-159). Hoboken, New Jersey: Wiley.
13. ASTM D6342-12, (2012). *Standard Practice for Polyurethane Raw Materials: Determining Hydroxyl Number of Polyols by Near Infrared (NIR) Spectroscopy*, West Conshohocken, PA: ASTM International, [www.astm.org](http://www.astm.org).
14. *Near-infrared analysis of polyols*; Near-Infrared Spectroscopy Application Note NIR-6 for Metrohm: Riverview, FL.
15. *The Determination of OH Number in Polyols Using FT-NIR Spectroscopy*; FT-NIR Spectroscopy Application Note for PerkinElmer Instruments: Norwalk, CT, 2000.
16. Nikje, M.M.A., Abedinifar, F., & Idris, A. (2011). Epoxidized Soybean Oil Ring Opening Reaction under MW Irradiation; *Applied Science Research*. 3. 383-388.
17. Badri, K. H. (2012). *Biobased Polyurethane from Palm Kernel Oil-Based Polyol*; Polyurethane; Zafar, F., Sharmin, E., Eds.; InTech: Rijeka, Croatia. 447-455.
18. Dworakowska, S., Dariusz, B., & Prociak, A. (2010). Synthesis of polyols from rapeseed oil. Presented at ECSOC-14 [Online], CO12. Electronic Conference on Synthetic Organic Chemistry. [https://www.usc.es/congresos/ecsoc/14/hall\\_c\\_MAS/c012/index.pdf](https://www.usc.es/congresos/ecsoc/14/hall_c_MAS/c012/index.pdf). (accessed July 14, 2015).